

This discussion paper is/has been under review for the journal Atmospheric Chemistry and Physics (ACP). Please refer to the corresponding final paper in ACP if available.

Atmospheric impacts of the 2010 Russian wildfires: integrating modelling and measurements of the extreme air pollution episode in the Moscow megacity region

I. B. Konovalov^{1,2}, M. Beekmann², I. N. Kuznetsova³, A. Yurova³, and A. M. Zvyagintsev⁴

¹Institute of Applied Physics, Russian Academy of Sciences, Nizhniy Novgorod, Russia

²Laboratoire Inter-Universitaire de Systèmes Atmosphériques, CNRS UMR 7583, Université Paris-Est and Université Paris 7, Créteil, France

³Hydrometeorological Centre of Russia, Moscow, Russia

⁴Central Aerological Laboratory, Dolgoprudny, Russia

Received: 15 March 2011 – Accepted: 13 April 2011 – Published: 19 April 2011

Correspondence to: I. B. Konovalov (konov@appl.sci-nnov.ru)

Published by Copernicus Publications on behalf of the European Geosciences Union.

Atmospheric impacts of the 2010 Russian wildfires

I. B. Konovalov et al.

Title Page

Abstract

Introduction

Conclusions

References

Tables

Figures

◀

▶

◀

▶

Back

Close

Full Screen / Esc

Printer-friendly Version

Interactive Discussion



Abstract

Numerous wildfires provoked by an unprecedented intensive heat wave caused continuous episodes of extreme air pollution in several Russian cities and densely populated regions, including the Moscow megacity region. This paper analyzes the chemical evolution of the atmosphere over the Moscow region during the 2010 heat wave by integrating available ground based and satellite measurements with results of meso-scale modeling. The state-of-the-art CHIMERE CTM is used, which is modified to take into account air pollutant emissions from wildfires and the shielding effect of smoke aerosols. The wild fire emissions are derived from satellite measurements of the fire radiative power and are optimized by assimilating data of ground measurements of carbon monoxide (CO) and particulate matter (PM₁₀) into the model. It is demonstrated that the optimized simulations reproduce independent observations, which were withheld during the optimisation procedure, quite adequately (specifically, the correlation coefficient of daily time series of CO and PM₁₀ exceeds 0.8) and that inclusion of the fire emissions into the model significantly improves its performance. The results of the analysis show that wildfires were a principal factor causing the observed air pollution episodes associated with the extremely high level of daily mean CO and PM₁₀ concentrations (up to 10 mg m⁻³ and 700 µg m⁻³ in the averages over available monitoring sites, respectively) in the Moscow region, although accumulation of anthropogenic pollution was also favoured by a stagnant meteorological situation. In contrast, diagnostic model runs indicate that ozone concentrations could reach very high values even without fire emissions which provide “fuel” for ozone formation, but, at the same time, inhibit it as a result of absorption and scattering of solar radiation by smoke aerosols. The analysis of MOPITT CO measurements and of corresponding simulations indicates that the observed episodes of extreme air pollution in Moscow were only a part of a very strong perturbation of the atmospheric composition, caused by wildfires, over the largest part of European Russia. It is estimated that 2010 fires in the European part of Russia emitted ~9.7 Tg CO, that is more than 85% of the total annual anthropogenic

Atmospheric impacts of the 2010 Russian wildfires

I. B. Konovalov et al.

Title Page

Abstract

Introduction

Conclusions

References

Tables

Figures



Back

Close

Full Screen / Esc

Printer-friendly Version

Interactive Discussion



CO emissions in this region. About 30% of total CO fire emissions in European Russia are identified as emissions from peat fires.

1 Introduction

An unprecedented intensive heat wave provoked thousands of wildfires during summer of 2010 over European Russia. These fires had devastating consequences for forests, crops, and infrastructure (2010 Russian wildfires, 2011). Continuous episodes of severe air pollution were observed during this period in several Russian regions and large cities, including Moscow, Nizhniy Novgorod, Ryazan, Tula, Vladimir and Voronezh. The state of emergency was officially declared during these events in seven Russian regions.

From a scientific point of view, the extreme perturbation of atmospheric parameters in summer 2010 over European Russia provided a critical test for the current understanding of atmospheric processes as well as for atmospheric and climate models. Among numerous issues raised by this phenomenon, this paper focuses on the analysis of extreme air pollution episodes observed in the Moscow megacity region. The Moscow region is a highly urbanized territory with a total population exceeding 15 millions of inhabitants. Moscow is the Russian capital and the largest city in Europe. It is one of the major political, economic, cultural, and transportation centers of Europe and the world. Similar to many other megacities (Molina and Molina, 2004), Moscow experiences serious environmental problems, including air pollution (Zvyagintsev et al., 2004; Gorchakov et al., 2006; Konovalov et al., 2009; Kuznetsova et al., 2011), even under normal conditions. For this reason, although the contribution of wildfires to the observed extreme air pollution experienced by Moscow's inhabitants in summer 2010 was likely predominant, the role of anthropogenic factors might also be important and could not be a priori neglected in a quantitative analysis.

Modeling of air pollution caused by predominantly anthropogenic sources has been a subject of a vast number of studies. Although the performance of the state-of-the-art

Atmospheric impacts of the 2010 Russian wildfires

I. B. Konovalov et al.

Title Page

Abstract

Introduction

Conclusions

References

Tables

Figures

◀

▶

◀

▶

Back

Close

Full Screen / Esc

Printer-friendly Version

Interactive Discussion



chemistry transport models (CTMs) is yet far from being perfect, it was demonstrated (see, e.g., Vautard et al., 2007) that in many instances they are capable of reproducing and predicting important features of the observed evolution of major air pollutants. On the other hand, emissions from wild fires are usually not taken into account in standard configurations of most regional CTMs, and thus they are not directly applicable in situations where the role of wildfires may be significant. Meanwhile, there is a bulk of evidence that wildfires may have a strong impact on air quality (see, e.g., Langmann et al., 2009 and references therein). A major factor hampering progress in modeling effects of wildfires on air pollution is the lack of sufficiently accurate estimates of gaseous species and aerosol emissions from these fires.

Available methods to obtain fire emission estimates have been discussed in numerous papers. A most common approach to derive fire emissions is based on the use of information on the burned area (e.g., Seiler and Crutzen, 1980; Crutzen and Andreae, 1990; Andreae and Merlet, 2001; Hao et al., 1996; van der Werf et al., 2006, 2010; Jain et al., 2006). Apart from the burned area estimates which, in recent years, have become available from satellite measurements (e.g., Grégoire et al., 2003; Giglio et al., 2006), this approach requires additional data characterizing the local biome and the available fuel load, which, in many instances, are rather uncertain. Global fire emission inventories developed with this approach are mainly designed for global atmospheric and climate models and are not directly suitable for regional CTM because of too low temporal and spatial resolution (e.g., the Global Fire Emissions Database, GFED3, created by van der Werf et al., 2010, provides data with a monthly time step and a special resolution of 0.5°), although it has been proposed (Pfister et al., 2005; Wiedinmyer et al., 2006; Wang et al., 2006) that a temporal resolution of fire emissions can be increased by using satellite observations of thermal anomalies (Giglio et al., 2003).

An alternative approach to obtain fire emission estimates is based on a direct empirical relationship between fire radiative power (FRP) retrieved from satellite measurements and the instantaneous rate of biomass burning (Ichoku and Kaufman, 2005;

Atmospheric impacts of the 2010 Russian wildfires

I. B. Konovalov et al.

Title Page

Abstract

Introduction

Conclusions

References

Tables

Figures



Back

Close

Full Screen / Esc

Printer-friendly Version

Interactive Discussion



Wooster et al., 2005). An important advantage of this approach is its applicability in near real time data assimilation systems (Sofiev et al., 2009; Kaiser et al., 2009). It also allows avoiding potentially large uncertainties associated with estimates of available fuel load. In this study, we follow this approach, having in mind prospects of operational applications of our modeling system for air quality forecasts and air pollution control in Russia (Kuznetsova et al., 2010).

Wildfire emission estimates obtained by different methods have been used in many modeling studies addressing atmospheric effects of wildfires at global and continental scales. For example, Park et al. (2003) used the global GEOS-CHEM model to simulate seasonal evolution of carbonaceous aerosols over the United States and to estimate their sources. The same model was used by Jaffe et al. (2004) and Jeong et al. (2008) with biomass burning emissions estimated with monthly temporal resolution in order to study effects of Siberian forest fires on air quality in East Asia. Turquety et al. (2007) used the GEOS-CHEM model and daily inventory of wildfire emissions to simulate the evolution of carbon monoxide over North America and to identify the role of peat burning. Pfister et al. (2008) employed the MOZART global model to study the impacts of Californian wildfires on surface ozone in US. The IMAGES global CTM was used by Stavrou et al. (2009) to evaluate available estimates of pyrogenic emissions of non-methane volatile organic compounds.

The reduction of potential uncertainties in global model results can be achieved by averaging global model output over sufficiently large areas and/or long (e.g., monthly) time periods. This way would not be practical in the case of regional air pollution models, as they are expected to address much finer temporal and spatial scales dictated by the necessity to simulate regional air pollution episodes. Accordingly, more accurate emission data are typically needed in the case of regional CTM. It is not surprising then that comparisons of simulations performed by regional CTMs employing wildfire emission data with air pollution measurements have so far been presented in very few papers. Specifically, Wang et al. (2006) used the Regional Atmospheric Modeling System (RAMS) which did not include atmospheric chemistry and secondary aerosol

Atmospheric impacts of the 2010 Russian wildfires

I. B. Konovalov et al.

Title Page

Abstract

Introduction

Conclusions

References

Tables

Figures

◀

▶

◀

▶

Back

Close

Full Screen / Esc

Printer-friendly Version

Interactive Discussion



**Atmospheric impacts
of the 2010 Russian
wildfires**

I. B. Konovalov et al.

Title Page

Abstract

Introduction

Conclusions

References

Tables

Figures



Back

Close

Full Screen / Esc

Printer-friendly Version

Interactive Discussion



formation to simulate the transport of smoke aerosols from Central America to US. A particular goal of their study was to examine the impact of including diurnal variations of fire behavior on smoke transport simulated by RAMS. They found that the simulated aerosol concentrations correlate well with corresponding monitoring data but are much smaller than observations. Unexpectedly, they found also that including diurnal variations of wildfire emissions did not improve the agreement between simulations and measurements. Hodzic et al. (2007) compared aerosol optical properties simulated by the CHIMERE CTM with those derived from the MODIS and POLDER satellite measurements. They demonstrated the ability of the model to adequately reproduce perturbations of aerosol optical thickness (AOT) caused by the advection of a smoke plume from the source region in Portugal to Northern Europe. However, inclusion of fire emissions in the model did not allow improving temporal variability of AOT data at specific locations of the AERONET monitoring network. Larkin et al. (2009) presented a modeling framework enabling simulations of the cumulative smoke impacts from fires across the USA. They showed that the modeled output generally compares well with satellite plume observations, but underpredicts measured $PM_{2.5}$ concentrations during the considered episode. While Wang et al. (2006), Hodzic et al. (2007) and Larkin et al. (2009) used wildfire emission inventories based on the burnt area approach, Sofiev et al. (2009) derived aerosol fire emissions from FRP measurements. Their emission estimates were then used in the SILAM CTM to simulate $PM_{2.5}$ concentrations and columns. They have demonstrated some similarity of spatial distributions in simulations and measurements during selected episodes of intensive fires in Europe, but the temporal evolution of the simulated $PM_{2.5}$ concentrations and columns was not quantitatively evaluated.

Here we examine the feasibility of using pyrogenic emission estimates derived from satellite FRP measurements to simulate air pollution in a megacity region during a period of intensive wildfires during the heat wave of summer 2010. The important features of the situation addressed in this study are strongly perturbed (by smoke) optical properties of the atmosphere and significance of peat fires. These features make direct

estimation of fire emissions from FRP difficult, and ways to overcome these difficulties are proposed. One of the ideas exploited in this study is to use an inverse modeling approach to optimize scaling factors used to convert FRP to the biomass burning rate. We also evaluate the impact of wildfires on air quality in the Moscow megacity region during this period. A distinctive feature of this study is a parallel analysis of the evolution of several major pollutants of both primary and secondary origin (CO, PM₁₀, O₃). Such an approach allows us not only to evaluate wildfire emission estimates, but also to examine the ability of a state-of-the-art CTM to simulate complex processes driving formation of secondary pollutants in a strongly polluted atmosphere.

2 Measurement data

2.1 Satellite measurements

2.1.1 Fire radiative power (FRP)

FRP is retrieved from the measurements performed by MODIS (Moderate Resolution Imaging Spectroradiometer) instruments on board of NASA Aqua and Terra satellites (Ichoku and Kaufmann, 2005). The nominal resolution of FRP measurements by MODIS is about 1 km². The polar orbiting Aqua and Terra satellites overpass the same region in the middle latitudes twice a day.

We used the standard MODIS data products, which are publicly distributed by the Land Processes Distributed Active Archive Center (LP DAAC) through the Earth Observing System Clearing House (ECHO, <http://www.echo.nasa.gov/>) system as Level 2 (orbital) and Level 3 (gridded) products. The algorithm of FRP retrieval (Kaufmann et al., 1998) is based on an empirical relationship between FRP and temperature measured at the 4 μm MODIS channel in a pixel with fires and an adjacent “background” pixel without fires (T_{4f} and T_{4b} , respectively):

$$\text{FRP} \cong 4.34 \times 10^{-13} \left(T_{4f}^8 - T_{4b}^8 \right) \text{ [Watt]} \quad (1)$$

Atmospheric impacts of the 2010 Russian wildfires

I. B. Konovalov et al.

Title Page

Abstract

Introduction

Conclusions

References

Tables

Figures

◀

▶

◀

▶

Back

Close

Full Screen / Esc

Printer-friendly Version

Interactive Discussion



Atmospheric impacts of the 2010 Russian wildfires

I. B. Konovalov et al.

Title Page

Abstract

Introduction

Conclusions

References

Tables

Figures

◀

▶

◀

▶

Back

Close

Full Screen / Esc

Printer-friendly Version

Interactive Discussion



This dependence was obtained by fitting the simulated energy released from many pixels with fires as a function of average radiance at 4 μm . Each pixel contained 500 zones with different physical temperature representing both smoldering and flaming fires, and the standard deviation in the derived fire energy is estimated as 16% on the average (Kaufmann et al., 1998). However, there are many factors that may lead to much larger uncertainties in real FRP measurement data. Among these factors are clouds and aerosols that may attenuate infrared radiation detected by a satellite instrument and dilute the contrast between the background and fire pixels. Estimation of FRP from space is especially difficult or impossible for fires overshadowed by trees and for sub-surface smoldering fires (peat fires). All these factors may cause negative biases in the FRP retrievals.

The polar orbiting Aqua and Terra satellites cannot provide sufficient information about the diurnal cycle of fire activity. For this reason, a fixed diurnal profile of FRP, $\rho_h(t)$, is assumed, which was adopted from WRAP (2005) (see Fig. 1). The same profile was used by Hodzic et al. (2007).

The Level 2 FRP data (MOD14/MYD14) were projected to a regular grid (with a resolution of $0.2^\circ \times 0.1^\circ$ for longitude and latitude). This resolution corresponds to that of our model grid employed for regional-scale simulations. Specifically, for each orbit k we defined a spatially averaged FRP density, Φ_k , corresponding to a given cell of the output grid as follows:

$$\Phi_k = \frac{\sum_j \text{FRP}_{jk}}{\sum_j S_{jk}^f + S_k^c}, \quad (2)$$

where j is the index of an observed pixel falling into the grid cell i , FRP_k and S_{jk}^f are FRP (MW) and the area (km^2) of the fire pixel, respectively, and S_k^c is the total observed area of the surface (in the considered grid cell) identified in MODIS measurements as water and non-fire clear land. An area, for which observational information about potential fire activity is not retrieved (because of clouds or any other reasons), is not taken

into account in S_k^c . To avoid technical difficulties associated with obtaining and processing of huge amount of geolocation data needed to estimate S_k^c from Level 2 data, we have derived S_k^c from the Level 3 daily data product (MOD14A1/MYD14A1) provided on a $1 \times 1 \text{ km}^2$ grid. This simplification may entail some random uncertainties in Φ due to possible inconsistencies between the observed area identified at a given overpass of a satellite and the area reported in the daily data product. However, this kind of a possible error is hardly significant in comparison with other inevitable uncertainties in the measured FRP data.

The goal of the next step is to obtain estimates for daily mean values of FRP, Φ_d . One possibility is averaging all FRP orbital data available for a given day. However, we have found that this way leads to strongly underestimated (by more than an order of magnitude) emissions of air pollutants, probably because of the contribution of scenes partly obscured by clouds but not entirely disregarded in the FRP retrievals. Instead, only a maximum value among values of Φ_k observed in a given grid cell and during a given day d is taken into account:

$$\Phi_d = \max \{ \Phi_k, k = 1, \dots, K \} \rho_h(t_{\max})^{-1} \quad (3)$$

where K is the total number of scans during the given day, and $\rho_h(t_{\max})$ is the weighting factor accounting for the assumed diurnal variation of FRP; t_{\max} is the moment when the scan with the maximum FRP was done.

2.1.2 Aerosol optical depth (AOD)

Similar to the FRP data described above, the AOD data used in this study are retrieved from measurements performed by the MODIS satellite instrument. Specifically, we make use of the aerosol optical depths at 550 nm provided as the Level 3 daily data (MYD08_D3) gridded with a spatial resolution of $1 \times 1^\circ$. In this study, grid cells with missing data are filled in by spatial averaging over an area of 5 by 5° . For the period considered in this study, only AQUA AOD measurements were available. A description of the retrieval procedure can be found in Kaufmann et al. (1997). The estimated

Atmospheric impacts of the 2010 Russian wildfires

I. B. Konovalov et al.

Title Page

Abstract

Introduction

Conclusions

References

Tables

Figures

◀

▶

◀

▶

Back

Close

Full Screen / Esc

Printer-friendly Version

Interactive Discussion



relative uncertainty of the MODIS AOD data over land is about 20% and the absolute part of errors ranges within ± 0.05 (Ichoku et al., 2005).

2.1.3 CO mixing ratio

We use CO mixing ratios derived from infrared radiance measurements which are performed by the MOPITT instrument onboard the NASA Terra satellite. The MOPITT retrievals (version V4) include CO mixing ratio for a floating surface level followed by nine uniformly spaced levels from 900 to 100 hPa. Only data for 900 hPa pressure level are considered in this study. It should be noted that the information provided in the MOPITT data product for the given level actually comes from all levels although with different weights specified by the corresponding averaging kernels (see, e.g., Pfister et al., 2004). In other words, the retrieved mixing ratios at any level are a result of a certain non-uniform transformation of the actual vertical distribution of the CO mixing ratio. We use the Level 3 daily data (MOP03) given on a $1^\circ \times 1^\circ$ grid. Only daytime data are considered in this study because they provide more information about boundary layer processes simulated by our model.

2.2 Ground based measurements

We use measurements of CO, PM₁₀ and O₃ near-surface concentrations in the Moscow region, which were made at automatic monitoring stations of the State Environmental Institution “Mosecomonitoring”. The nominal measurement frequency was three measurements per hour. The network is equipped with modern analytical tools from leading producers (such as Teledyne Monitor Labs, Monitor Europe, Thermo Electron Corporation and others). Infrared spectrometry, ultraviolet fluorescence and TEOM methods were used for measurements of carbon monoxide, ozone and particulate matter, respectively. Most of the monitoring sites are located within boundaries of Moscow city, but there are also a few sites in Moscow suburbs (specifically, in

Atmospheric impacts of the 2010 Russian wildfires

I. B. Konovalov et al.

Title Page

Abstract

Introduction

Conclusions

References

Tables

Figures

◀

▶

◀

▶

Back

Close

Full Screen / Esc

Printer-friendly Version

Interactive Discussion



Zvenigorod, Zelenograd, and Pavlovskii Posad). Further information about the Mosecomonitoring air pollution monitoring network can be found on web (www.mosecom.ru).

The selection of monitoring sites considered in this study was based on their spatial representativeness and the total number of available measurements. Specifically, we consider only “residential” and “background” monitors providing more than 50% of days with the measurements during the analyzed period (from 1 June to 31 August). Road traffic and industrial sites are excluded from analysis. The total numbers of selected monitoring sites are 17, 7, and 8 for CO, PM₁₀, and O₃, respectively. Additionally, sites measuring CO and PM₁₀ were distributed randomly into two groups. One group is used for optimization of wildfire emissions used in our model, while the other is used only for validation of simulations. The groups used for optimization include respectively 9 and 4 CO and PM₁₀ monitors. O₃ measurements were not used in the optimization procedure; therefore, all measurement data from the selected O₃ monitors were used for validation.

To simplify our analysis, we consider time series of daily mean CO and PM₁₀ concentrations averaged over all sites in a given group. This is a logical approach in our case, taking into account that most of the monitors are situated within 20 km from the Moscow center and that this study does not address spatial variations of pollutant concentrations inside of the Moscow agglomeration.

Ozone concentrations measured in Moscow exhibit very strong spatial variability on fine scales (probably as a result of ozone titration by strong NO emissions in Moscow) which cannot be adequately addressed by our model. In such a situation, the model is expected to better predict the largest ozone concentration over the region than a spatially averaged concentration. It should also be taken into account that the model provides outputs on the hourly basis and the air quality standards in Russia regulate the daily maximum ozone concentration with the threshold value of 60 μg m⁻³. Accordingly, we construct a time series of daily values of measured ozone concentrations by selecting (for each day) a site with the largest daily maximum of 1-h mean ozone concentrations.

Atmospheric impacts of the 2010 Russian wildfires

I. B. Konovalov et al.

Title Page

Abstract

Introduction

Conclusions

References

Tables

Figures

⏪

⏩

◀

▶

Back

Close

Full Screen / Esc

Printer-friendly Version

Interactive Discussion



3 Simulations

3.1 CHIMERE chemistry transport model: general description and numerical experiment settings

We used the CHIMERE chemistry transport model (V2007), which is a multi-scale three-dimensional model designed to simulate air pollution in the boundary layer and free troposphere at regional and continental scales. Evaluation and description of the initial version of this model was presented by Schmidt et al. (2001). Since then the model has been used in numerous studies (e.g., Hodzic et al, 2005, 2007; Vautard et al., 2007; Bessagnet et al., 2008; Menut et al., 2009; Konovalov et al., 2008, 2010; Rouil et al., 2009; Beekmann and Vautard, 2010), while the model code permanently undergoes further developments and modifications. Along with sufficiently comprehensive (although simplified) representations of atmospheric gas-phase chemistry and transport, the model includes parameterisations of major processes driving formation and evolution of organic and inorganic aerosols (such as nucleation, condensation, coagulation, dry and wet deposition and saltation). An in-detail description of the model can be found in the CHIMERE technical documentation available on the web (<http://www.lmd.polytechnique.fr/chimere/>).

In this study, simulations were performed using a nested-domain approach. Specifically, we used a large domain covering both Western and Eastern Europe with a coarse resolution of $1^\circ \times 1^\circ$ and a small (nested) domain covering only several European regions of Russia (including the Moscow region) with the finer resolution of $0.2^\circ \times 0.1^\circ$. Simulations of the atmospheric composition by CHIMERE over Eastern Europe were evaluated earlier (Konovalov et al., 2005, 2009, Kuznetsova et al., 2010, 2011). It was found, in particular, that in spite of potentially large uncertainties in the anthropogenic emission inventory data (Vestreng, 2004) for Eastern Europe, CHIMERE demonstrates similar performance in both Western and Eastern parts of Europe (Konovalov et al., 2005). In the vertical dimension, the simulations were performed with 12 vertical levels specified in hybrid coordinates with the resolution decreasing from bottom to top

Atmospheric impacts of the 2010 Russian wildfires

I. B. Konovalov et al.

Title Page

Abstract

Introduction

Conclusions

References

Tables

Figures

◀

▶

◀

▶

Back

Close

Full Screen / Esc

Printer-friendly Version

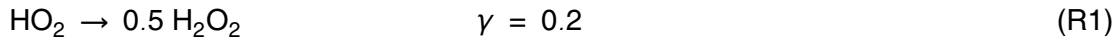
Interactive Discussion



in accordance with a geometrical progression. The top of the CHIMERE vertical domain is fixed at the 200 hPa pressure level. Boundary conditions for gaseous and aerosol species are specified by using monthly average (“climatological”) values of the MOZART (Horowitz et al., 2003) and GOCART (Ginoux et al., 2001) models, respectively.

Meteorological input data were calculated off-line with a horizontal resolution of $100 \times 100 \text{ km}^2$ using the MM5 non-hydrostatic meso-scale model (<http://www.mmm.ucar.edu/mm5/>). MM5 was initialised with NCEP Reanalysis-2 data (http://www.cpc.ncep.noaa.gov/products/wesley/ncep_data/). Possible effects of perturbations in the atmospheric radiative balance due to changes in atmospheric composition (in particular due to the large aerosol content owing to fires) could not be properly addressed in our modelling scheme. In a less direct way, they were taken into account in the NCEP Reanalysis-2 data through assimilation of measured data.

Simulations were performed with the MELCHIOR1 gas phase chemical mechanism (Lattuati, 1997) which includes more than 300 reactions of 80 species. Along with the gas phase chemical processes, a minimal set of heterogeneous reactions recommended by Jacob (2000) is considered in the standard version of the model with associated uptake coefficients given by Harrison and Kito (1990) and other references in Jacob (2000):



A simple parameterisation of reaction rates is used, following formulations of Aumont et al. (2003). It should be taken into account, however, that these formulations along with the parameters indicated above are mainly applicable to urban aerosols and probably

Atmospheric impacts of the 2010 Russian wildfires

I. B. Konovalov et al.

Title Page

Abstract

Introduction

Conclusions

References

Tables

Figures

◀

▶

◀

▶

Back

Close

Full Screen / Esc

Printer-friendly Version

Interactive Discussion



should be revised in the case of fire aerosols. Moreover, major modifications of the simple parameterization of heterogeneous processes in CHIMERE are needed in view of recent experimental findings (Monge et al., 2010) revealing that heterogeneous processes are strongly affected by solar radiation. Accordingly, as a conservative option for the base case simulations, we disregarded all heterogeneous reactions, although the impact of heterogeneous processes on atmospheric composition in our case could not be disregarded a priori. To get some idea about the potential role of heterogeneous reactions in the presence of high aerosol concentration, we performed a model test run (see Sect. 5.3) with the “standard” parameterization of the heterogeneous Reactions (R1)–(R4).

Calculations of photolysis rates in the model are based on the tabulated outputs from the Troposphere Ultraviolet and Visible (TUV) model (Madronich et al., 1998) and depend on altitude, zenith angle and estimated optical thickness of clouds. The aerosol impact on photolysis rates, potentially significant in a polluted atmosphere (see, e.g., Dickerson et al., 1997; Martin et al., 2003; Hodzic et al., 2007) has not yet been taken into account in the CHIMERE standard version. In this study, optical effects of smoke aerosols are roughly taken into account by means of a simple observation-based approach, combined to output from explicit modelling. Specifically, we estimate the photolysis rates (J_a) at the surface in the presence of aerosols as a function of the effective aerosol optical depth:

$$J_a = J_s \exp(-\gamma \text{AOD}_{\text{modis}}) \quad (4)$$

where J_s are the photolysis rates evaluated in CHIMERE, $\text{AOD}_{\text{modis}}$ is the aerosol optical depth at 550 nm (from MODIS measurements, see Sect. 2.1.2), and γ is the conversion factor specified as a function of the solar zenith angle. The photolysis rates at an arbitrary altitude are calculated similar to Eq. (4) but under an additional assumption that most aerosol particles are uniformly distributed either within the boundary layer if the boundary layer height is larger than the maximum injection height for smoke aerosols (see below), or up to the maximum injection height otherwise. The

**Atmospheric impacts
of the 2010 Russian
wildfires**

I. B. Konovalov et al.

Title Page

Abstract

Introduction

Conclusions

References

Tables

Figures

◀

▶

◀

▶

Back

Close

Full Screen / Esc

Printer-friendly Version

Interactive Discussion



dependence of γ on the zenith angle is approximated (see Fig. 2) by using explicit calculations performed by Hodzic et al. (2007, Fig. 10) with the TUV model in the case of the NO_2 photolysis rate under the assumption that a single scattering albedo (SSA) of aerosol particles equals to 0.8 (this value was assumed to be representative of biomass burning aerosols, taking into account measurements of SSA values reported by Meloni et al., 2006). A value of γ is assumed to increase in accordance to the equation depicted in Fig. 2 as $\cos(\varphi)$ decreases to 0.01 and remains constant afterwards. The wavelength dependence of γ is disregarded.

Anthropogenic emissions are based on the “expert” annual data of the EMEP emission inventory (UNECE, 2009; EMEP, 2010) taken from the EMEP Centre on Emission Inventories and Projections (CEIP) website (<http://www.ceip.at/>) with the initial resolution of $0.5^\circ \times 0.5^\circ$. For the nested domain, emissions were downscaled proportionally to the population density (GPW, 2010). Higher resolution emission data from other European inventories (e.g., the TNO emission inventory) were tested with CHIMERE but did not yield any better agreement of simulations with monitoring data in Moscow than the downscaled EMEP data.

The estimation of pyrogenic emissions is described in Sect. 4. Here, the choice of the injection height is discussed. In our study, the maximum injection height of fire emissions is defined as a constant parameter. Such a highly simplified approximation of the actual injection height (which in the reality depends on the flaming intensity and meteorological conditions) is partly based on analysis presented by Sofiev et al. (2009). Specifically, by plotting measured values of the height of real smoke plumes as function of corresponding FRP, they have shown that the plume height was almost independent on FRP within the range of FRP values typical for European fires, and its values are quasi-randomly scattered in the range from about 100 m to 2 km. Based on these findings, the pyrogenic emissions are homogeneously distributed in the model up to 1 km. It is expected that if the boundary layer height (which is typically less than 2 km) exceeds 1 km, then the emissions are rapidly distributed within the boundary layer by turbulent mixing; otherwise, the pyrogenic emissions are expected to be injected

**Atmospheric impacts
of the 2010 Russian
wildfires**

I. B. Konovalov et al.

Title Page

Abstract

Introduction

Conclusions

References

Tables

Figures

◀

▶

◀

▶

Back

Close

Full Screen / Esc

Printer-friendly Version

Interactive Discussion



**Atmospheric impacts
of the 2010 Russian
wildfires**

I. B. Konovalov et al.

[Title Page](#)[Abstract](#)[Introduction](#)[Conclusions](#)[References](#)[Tables](#)[Figures](#)[◀](#)[▶](#)[◀](#)[▶](#)[Back](#)[Close](#)[Full Screen / Esc](#)[Printer-friendly Version](#)[Interactive Discussion](#)

above the boundary layer due to pyro-convection. In their own modelling study, Sofiev et al. (2009) used a similar simple approach by assuming that 50% of the emissions are injected in the lowest 200 m, and the rest is homogeneously distributed from 200 m up to 1 km. Different simple methods were used in other modeling studies addressing effects of fire emissions. For example, Turquety et al. (2007) tested several assumptions for the altitude of injection of North American fire emissions, including injection of all the emissions in the boundary layer, and injection of only 40% or 60% of emissions in the boundary layer. They did not find significant differences in comparisons of their simulations with MOPITT measurements over the whole period (three summer months of 2004) considered in their study, although they noted that releasing a significant fraction of emissions in the upper troposphere brought some improvements in simulations downwind from the source regions for the large transport events. In the framework of their inverse modeling study of CO fire emissions from Alaskan wildfires, Pfister et al. (2005) found that injecting CO only into the boundary layer gave almost the same results as distributing the fire emissions uniformly up to about 7 km.

Two fractions (fine and coarse ones) of aerosol emissions were distributed among 8 size bins with the diameter of particles ranging from 10 nm to 10 μ m in accordance to a bi-modal lognormal distribution. The parameters of this distribution were the same as in the study by Hodzic et al. (2007): a fine mode was centered on a 0.25 μ m mean diameter (1.6 geometric standard deviation) and a coarse mode was centered on a 5 μ m mean diameter (1.4 geometric standard deviation).

During this study, CHIMERE was run for the period from 28 May to 31 August 2010 using several different model configurations. Specifically, a model run was performed with fire emissions and with account for the shielding effects of aerosols (see Eq. 4) but without heterogeneous chemistry, as explained above. This simulation is referred to as the “FE” run and is considered as the base case in this study. To assess the direct effect of fire emissions on the atmospheric composition, the results of the FE run are compared with those of the reference run (which is referred to below as the REF run). The configuration of the REF run is the same as that of the FE run, except that fire

emissions are set to be zero. Other model configurations considered in this study are defined in Sect. 5.3. The model runs performed in this work are summarized in Table 1.

3.2 Initial processing of model results

The “raw” results of model runs were processed to insure their consistency with measurements used for their evaluation. To compare simulations of near surface concentrations with the air pollution monitoring data, the hourly concentrations at the lowest model level were first extracted from the model output files for each grid cell whose center is closest to the location of a corresponding monitoring site. Then the hourly concentrations were either averaged over twenty-four hours (for CO and PM₁₀), or the daily maximum concentration was determined (for ozone).

A more complicated processing of model results was needed for their comparison with the MOPITT CO measurements. Specifically, as recommended by Deeter et al. (2009), we took into account the sensitivity of the retrieved CO vertical profile to the true CO vertical distribution by means of a logarithmic transformation of the modeled profile:

$$\text{Log}(\mathbf{x}_{\text{st}}) = \text{Log}(\mathbf{x}_{\text{so}}) + \mathbf{A} [\text{Log}(\mathbf{x}_{\text{so}}) - \text{Log}(\mathbf{x}_{\text{a}})] \quad (5)$$

where \mathbf{x}_{so} and \mathbf{x}_{st} are the simulated CO profiles before and after the transformation, \mathbf{x}_{a} is the a priori CO profile, and \mathbf{A} is a matrix of the averaging kernels. The transformation Eq. (5) was applied to the simulated CO concentrations in each grid cell and for each hour. Because the exact time of the MOPITT scans (which considerably varies from day to day) is not reported in the MOPITT CO Level 3 (daytime) data product used in this study, the transformed CO concentrations are averaged over the period from sunrise to sunset. We found that the transformed CO data are quite insensitive to the definition of the averaging period, and that possible biases caused by a probable temporal mismatch between measurements and simulations cannot account for the differences between the measured and simulated CO mixing ratios discussed in Sect. 5.4.

Atmospheric impacts of the 2010 Russian wildfires

I. B. Konovalov et al.

Title Page

Abstract

Introduction

Conclusions

References

Tables

Figures

◀

▶

◀

▶

Back

Close

Full Screen / Esc

Printer-friendly Version

Interactive Discussion



4 Estimation of air pollutant emissions from wildfires

4.1 Basic formulations

The fire emission estimates are obtained in this study by assuming a linear relationship between the biomass burning rate and FRP. Such a relationship was identified by Wooster et al. (2005) in measurements of experimental fires. However, taking into account that the experiments could not reproduce a very wide range of real burning conditions, the actual relationship between the wildfire emissions and the FRP may be much more complex than assumed, and the estimation algorithm described below should be considered as a heuristic procedure.

In this study, the emission rates of gaseous species and particulate matter from wildfires in a given grid and at a given hour, t , are calculated as follows:

$$E_s(t) \cong \Phi_d \times \alpha \times (\beta_{sl} \times F_1 + \beta_{sp} \times \rho \times F_2) \times C(\tau) \times \rho_h(t), \quad (6)$$

where E_s ($\text{g s}^{-1} \text{m}^{-2}$) is the emission rate of a model species s , Φ_d (W m^{-2}) is the FRP density (or, in other words, the flux of infrared radiation) derived from satellite measurements (see Eqs. 2 and 3), α ($\text{g}[\text{organic matter}] \text{s}^{-1} \text{W}^{-1}$) is the empirical coefficient transforming the FRP density into the combustion rate density, β_{sl} ($\text{g}[\text{model species}]/\text{g}[\text{biomass}]$) is the emission factor for a given type l (or ρ) of the land cover, ρ is a fraction of peatland area in a given grid cell, $F_{1,2}$ are scaling factors optimized in model runs, ρ_h is the assumed diurnal profile of emissions (see Fig. 1), and C in an additional correction factor (see below) specified as a function of the aerosol optical thickness, τ .

We consider nine different land types defined in the CHIMERE CTM used in this study. The fractions of land cover per grid cell are evaluated using Global Land Cover Facility (GLCF) data base (<http://www.landcover.org>). The land cover types used in CHIMERE and their correspondence to the GLCF data is described in the CHIMERE CTM documentation available on the web (<http://www.lmd.polytechnique.fr/chimere/>). Additionally, we consider the “peatland” category of the land cover by introducing a

Atmospheric impacts of the 2010 Russian wildfires

I. B. Konovalov et al.

Title Page

Abstract

Introduction

Conclusions

References

Tables

Figures

◀

▶

◀

▶

Back

Close

Full Screen / Esc

Printer-friendly Version

Interactive Discussion



**Atmospheric impacts
of the 2010 Russian
wildfires**

I. B. Konovalov et al.

Title Page

Abstract

Introduction

Conclusions

References

Tables

Figures

◀

▶

◀

▶

Back

Close

Full Screen / Esc

Printer-friendly Version

Interactive Discussion



fraction (ρ) of the land surface identified as the peatland. This complication allows us to take into account, in an indirect way, emissions from peat fires. Although peat fires cannot be directly detected from satellites, we expect that if a crown or surface fire is observed over the dry peatland, there is some probability that a subsurface peat fire takes place at the same time. Note that a similar assumption was made by Turquety et al. (2007) in their modelling study of impacts of peat fires on carbon monoxide pollution of atmosphere over the USA. The peatland map for Russia on the grid of $0.9^\circ \times 0.72^\circ$ was obtained from the GIS “Peatlands of Russia” (Vompersky et al., 2005) (see Fig. 3). The coarse resolution of this map probably introduces additional uncertainties in emission estimates from peatfires, but taking into account that the assumed relation between FRP and the intensity of peatfires has a probabilistic character it is not at all obvious that further increase of the peatland map’s resolution would lead to significantly better emission estimates.

A value of α ($3.68 \times 10^{-4} \text{ g J}^{-1}$) has been adopted from the experimental study by Wooster et al. (2005). Emission factors for $\text{PM}_{2.5}$, PM_{10} , CO , NO_x , SO_2 , and NH_3 for different GLCF landuse types were adopted from Wiedinmyer et al. (2006). The total emissions of non-methane hydrocarbons (NMHCs) are evaluated by using the NMHCs emission factor given by Wiedinmyer et al. (2006), while data emission factors for individual hydrocarbons (Urbanski et al., 2009) are used to split total NMHCs into emissions of different model species.

In the case of peatland fires, the emission factors for CO , NO_x , and NH_3 are assigned using data of laboratory measurements (Yokelson, 1997; Christian et al., 2003) combined by Akagi et al. (2010). The emission factors evaluated by Akagi et al. (2010) for several hydrocarbons emitted from peat burning and grassland fires are used to obtain the NMHC emission factor for peat fires by scaling the corresponding factor reported by Wiedinmyer et al. (2006) for grassland. Due to the lack of direct measurements of $\text{PM}_{2.5}$ and PM_{10} emissions from peat burning, the emission factors for $\text{PM}_{2.5}$ and PM_{10} are assigned to be the same as for the grasslands, although probably they are much larger (Iinuma et al., 2007). Note that the results of this study are not sensitive to our

choices made for emission factors for particulate matter and CO because the pyrogenic emissions of these species are optimized using measurements (see Sect. 4.2). In contrast, the NMHCs emission estimates are not optimized in this study (but scaling for CO and PM emission factor is used), and so their accuracy can only be indirectly assessed by comparing simulated ozone concentrations with measurements. Taking into account that emission efficiency of actual fires may strongly depend on conditions of burning (e.g., Muraleedharan et al., 2000), which are not controlled in this study, values of emission factors assigned here (see Table 2) should only be considered as rough estimates.

Along with the scaling parameters F_1 and F_2 , our formulation for wildfire emissions (see Eq. 6) contains one more correction factor, C , which is assumed to depend on the aerosol optical thickness, τ . This is an ad hoc parameter introduced in order to account for possible underestimation of FRP from fires obscured by smoke aerosols. Heavy smoke is mentioned by Giglio (2010) among the main factors affecting accuracy of MODIS fire data products. Based on the limited number of numerical experiments, it was found that the agreement of model simulations with measurements drastically improves if $C(\tau)$ is defined as follows:

$$C(\tau) = \exp(\kappa \text{AOD}_{\text{modis}}) \quad (7)$$

where $\text{AOD}_{\text{modis}}$ is the aerosol optical depth at 550 nm, obtained with $1 \times 1^\circ$ resolution as a MODIS Level 3 data product provided from MODIS measurements (see Sect. 2.1.2) and κ is a constant which, in our simulations, was set to be unity. A methodical optimization of κ was not carried out. However, it was found in testing model runs that if κ is much smaller or much larger than unity then the model performance degrades. Therefore, setting κ to 1 is a heuristic choice which is justified (at least, to a certain degree) by numerical results. The simulations performed with $\kappa = 0$ and $\kappa = 1$ are compared in Sect. 5.3.

An idea behind the relation given by Eq. (7) is rather simple. As it is shown by Wooster et al. (2003, 2005), FRP derived from MODIS measurements using Eq. (1)

Atmospheric impacts of the 2010 Russian wildfires

I. B. Konovalov et al.

Title Page

Abstract

Introduction

Conclusions

References

Tables

Figures

◀

▶

◀

▶

Back

Close

Full Screen / Esc

Printer-friendly Version

Interactive Discussion



can alternatively be expressed as a linear function of the spectral radiance, L_f , emitted in the 3.4–4.2 μm wavelength range. The measured spectral radiance, $L_{f,\text{meas}}$, is attenuated by aerosols, such that

$$L_{f,\text{meas}} \approx L_{f,\text{true}} \exp(-\tau_4), \quad (8)$$

5 where $L_{f,\text{true}}$ and τ_4 are the true spectral radiance and aerosol optical thickness at the 4 μm wavelength, respectively. The measured FRP should be attenuated in a similar way. Since the measurements of τ_4 have not been available, we used $\text{AOD}_{\text{modis}}$ (with $1 \times 1^\circ$ resolution) as a substitute. Relating $\text{AOD}_{\text{modis}}$ and τ_4 is not easy, because not only optical properties of aerosols but also the spatial structure of τ_4 on fine scales
10 which are not captured by $\text{AOD}_{\text{modis}}$ data should be taken into account. For example, heavy smoke over a single fire could completely obscure it from a satellite sensor, but, at the same time, corresponding $\text{AOD}_{\text{modis}}$ value (representing a much larger territory) would not be significantly different from a background value. Accordingly, even though available measurements (Key, 2001) suggest that τ_4 is much smaller than AOD at
15 550 nm, we expect that in certain situations τ_4 may be as large as $\text{AOD}_{\text{modis}}$ or even larger. A more careful analysis of possible impacts of aerosols on FRP measurements goes beyond the scope of this paper.

4.2 Optimization procedure

Basically, the idea of the optimization procedure performed in the framework of this study is to find estimates of certain parameters of a model which provide the best
20 agreement of simulations with measurements. Note that this idea is akin to the general ideas behind both the inverse modeling (e.g. Enting, 2002) and data assimilation (Eskes et al., 1999; Elbern et al., 2007; Barbu et al., 2009) approaches. In this study, we attempt optimization of a parameter vector, F , which consists of only two components which are the scaling factors F_1 and F_2 (see Eq. 6). As a result, we not only
25 optimize the model performance but also obtain emission estimates that are consistent with available measurements. It should be kept in mind, however, that these estimates

Atmospheric impacts of the 2010 Russian wildfires

I. B. Konovalov et al.

Title Page

Abstract

Introduction

Conclusions

References

Tables

Figures

◀

▶

◀

▶

Back

Close

Full Screen / Esc

Printer-friendly Version

Interactive Discussion



are sufficiently accurate only if the modeled relationship between concentrations and emissions is correct, subject to some random uncertainties in model results. This is a common condition assumed in any inverse modeling study. On the other hand, the improvement of model performance resulting from parameter optimization can be considered as a self-sufficient goal, irrespectively of the physical meaning attributed to the optimized parameters. This goal is typical for data assimilation studies.

Our optimization algorithm is based on the “twin experiment” method. Specifically, we first performed the model run with both F_1 and F_2 equal to unity ($F_1 = F_2 = 1$). The next two runs were successively performed with F_1 value increased by 10% and with a similarly perturbed value of F_2 . The results of all these runs were used to estimate partial derivatives of CO and PM₁₀ concentrations with respect of F_1 and F_2 . Under the assumption that the relationships between CO and PM₁₀ concentrations and corresponding fire emissions are linear, the estimates of these derivatives allowed us to find the optimal parameter values, F_{opt} , providing a minimum of a cost function, J , which is defined as a mean square error (MSE) of the model:

$$F_{\text{opt}} = \arg \min (J); \quad J = \frac{1}{N} \sum_{i=1}^N (C_m^i - C_o^i - \Delta_\varepsilon)^2, \quad (9)$$

where C_m and C_o are the modeled and observed daily mean concentrations, respectively, i is the index of a day, N is the total number of days provided with observations and Δ_ε is a bias (systematic error) of the simulations. The bias is assumed to be independent of any processes caused by wildfire emissions and is estimated as a difference between the simulated and observed concentrations averaged over the period from 1 June to 15 July 2010. According to our simulations (see Sect. 5.2), the impact of wildfires on air pollution in Moscow during this period was indeed quite negligible. Technically, F_{opt} was found by resolving a system of two linear algebraic equations obtained by requiring that the partial derivatives of J with respect to F_1 and F_2 are equal zero. Different sets of optimal parameters were obtained for CO and particulate matter (PM), with the same correction factor applied to both fine and coarse fraction of aerosol.

**Atmospheric impacts
of the 2010 Russian
wildfires**

I. B. Konovalov et al.

Title Page

Abstract

Introduction

Conclusions

References

Tables

Figures

◀

▶

◀

▶

Back

Close

Full Screen / Esc

Printer-friendly Version

Interactive Discussion



**Atmospheric impacts
of the 2010 Russian
wildfires**

I. B. Konovalov et al.

[Title Page](#)[Abstract](#)[Introduction](#)[Conclusions](#)[References](#)[Tables](#)[Figures](#)[◀](#)[▶](#)[◀](#)[▶](#)[Back](#)[Close](#)[Full Screen / Esc](#)[Printer-friendly Version](#)[Interactive Discussion](#)

Evaluating potential uncertainties in optimal values of F_1 and F_2 is a difficult task requiring knowledge of the probability distributions of measurement and model errors. These uncertainties are expected to roughly express possible biases in the spatially and temporally averaged fire emissions. In the considered complex situation, there are many error components, such as, in particular, measurement (instrumental) errors, representativity errors caused by a limited spatial resolution of the model, errors in anthropogenic and natural emissions (including uncertainties in spatial and temporal structure of the wildfire emissions), uncertainties associated with chemical mechanism and parameterization of aerosol processes, and errors in boundary conditions. Each of these components may satisfy a different unknown probability distribution, and its contribution to differences between measurement and simulations may vary in both time and space. Accordingly, only very rough estimates of uncertainties in F_{opt} can be obtained without any detailed knowledge of all these factors.

To obtain such estimates, we performed a Monte Carlo experiment (see, e.g. Press et al., 1992). For this experiment, values of CO and PM₁₀ concentrations simulated with the optimal parameter values were considered as a substitute for the true values of these concentrations. Following a common approach used in inverse modeling studies (e.g., Tarantola, 1987), we do not discriminate between uncertainties in measurements and simulations but rather characterize all of them by introducing an effective observational error satisfying (in our case) a Gaussian probability distribution. The standard deviation, σ_ε of this probability distribution is evaluated as the root mean square deviation of the “true” concentrations from corresponding observations in the period of intensive wildfires in the Moscow region (from 20 July to 20 August). Choices of the type of probability distribution and of the period used to evaluate σ_ε are made in an attempt to best characterize actual uncertainties but they are nevertheless subjective. The errors sampled from the Gaussian distribution with the standard deviation σ_ε were applied to the substitutes of the true concentrations, and the estimation procedure defined by Eq. (9) was repeated with the randomly perturbed concentrations serving as substitutes for C_m . The sampling of random errors and the evaluation procedure were

re-iterated 1000 times to obtain the statistical distributions of logarithms of F_1 and F_2 . Finally, the geometric standard deviation corresponding to the 68.3 percentile of these distributions is calculated as a quantitative indicator of uncertainties in F_{opt} .

The optimization procedure employed in this study is relatively simple because not only any nonlinearities in relationships between concentrations of CO and PM₁₀ and their emissions from wildfires turned out to be small, but also the interaction between these species is rather negligible. In principle, changes in CO emissions can affect PM₁₀ concentrations through changes in chemical processes driving formation of secondary aerosols. However, in the considered situation with intensive wildfires, atmospheric aerosols are predominantly of primary origin. In turn, aerosol emissions can, in principle, affect CO concentration by modulating photolysis rates of many gaseous species which directly or indirectly interact with CO. However, the simulated aerosol concentrations were not used in this study for evaluation of radiative effects of aerosols. Instead, these effects were taken into account by using satellite AOD measurements, as described in Sect. 3.1. The legitimacy of a linear approximation for the relationships between CO (or PM₁₀) concentrations and corresponding wildfire emissions is confirmed by results of a comparison of CO and PM₁₀ concentrations estimated using a linear relationship between them and the wildfire emission factors and those simulated by CHIMERE with $F = F_{\text{opt}}$ (see Fig. 4). The efficiency of our simple optimization procedure is also directly manifested in results of comparison of optimized simulated concentrations with observations (see Sect. 5.2).

Optimized values of the factors F_1 and F_2 in the cases of CO and PM emissions are not directly applicable for the estimation of emissions of other model species, such as NO_x and NMHCs. If the emission factors β_s were known exactly, the optimal values of F_1 and F_2 would be the same for all species. Unfortunately, as it is demonstrated below, our optimization procedure yields rather different values in the cases of CO and PM, and this means that actual values of emission factors for different species in the considered fires might be significantly different from those assumed in our algorithm. In this situation, we have estimated emissions of all model species (except CO and

Atmospheric impacts of the 2010 Russian wildfires

I. B. Konovalov et al.

[Title Page](#)[Abstract](#)[Introduction](#)[Conclusions](#)[References](#)[Tables](#)[Figures](#)[◀](#)[▶](#)[◀](#)[▶](#)[Back](#)[Close](#)[Full Screen / Esc](#)[Printer-friendly Version](#)[Interactive Discussion](#)

assumed diurnal profile of fire emissions were uniform, values of F_1 and F_2 would be up to a factor of four larger. Note that uncertainties in our estimates of the correction factors not only depend on model and observations errors but also on the amount of available information allowing to resolve effects from peat fires and overground fires.

5 Not surprisingly, the uncertainties are much larger in F_2 than in F_1 estimates.

The estimates of wildfire emissions obtained using Eq. (6) with the optimized values of F_1 and F_2 are presented in Fig. 5 which shows spatial distributions of monthly mean CO fluxes from wildfires in comparison with seasonally averaged distributions of anthropogenic CO fluxes. The distributions are shown separately for the large European domain of CHIMERE and for the smaller (nested) domain covering only the Central European Russia (CER). It can be seen that while wildfire emissions in June were quite negligible with respect to anthropogenic emissions, they were very considerable in August. According to our estimates, wildfire emissions were strongest in the CER region, that is, not far from Moscow. Importantly, CO fluxes in certain regions (e.g.,
10 near Ryazan) were much larger than anthropogenic CO emissions from Moscow.

The estimates of total amounts of carbon monoxide emitted in different regions and months are listed in Table 4. Note that we cannot claim that our estimates concerning the European part of Russia or the whole Europe are sufficiently constrained by measurements, because measurements in Moscow are mainly sensitive to emissions in the CER region. In particular, values of physical parameters (such as α and β , see Eq. 6) describing the relationship between FRP and the emission rate may, in principle, be different in Western Europe from those in the CER region. For this reason, actual uncertainties in our total emissions may be different from those estimated in Monte Carlo experiment; the uncertainty ranges are thus not reported here. Nonetheless,
20 recognizing all possible uncertainties, we believe that our independent estimates are sufficiently adequate, and they can be useful for characterizing the global and regional impacts of 2010 Russian wildfires.

According to our estimates, the CER region provided the major part of total pyrogenic emission in Europe in August 2010. Moreover, only about 9% of the total European
25

Atmospheric impacts of the 2010 Russian wildfires

I. B. Konovalov et al.

Title Page

Abstract

Introduction

Conclusions

References

Tables

Figures

◀

▶

◀

▶

Back

Close

Full Screen / Esc

Printer-friendly Version

Interactive Discussion



amount of pyrogenic CO were emitted outside of Russia (mainly, in Portugal). Magnitudes of emissions are quite impressive: specifically, the total pyrogenic CO emissions in the European region of Russia (9.7 Tg) in summer 2010 constitute more than 85% of the total annual anthropogenic CO emissions in the same region (~ 11 Tg according to CEIP, <http://www.ceip.at/emission-data-webdab>). For comparison, the total amount of CO emitted during extreme fire events in Greece in August 2007 was reported to be about 0.3 Tg (Turquety et al., 2009). Interestingly, about 30% of total CO fire emissions in Russia are identified by our model optimization procedure as emissions from peat fires.

5.2 Comparative analysis of simulated and measured time series of air pollutant concentrations in the Moscow region

Figures 6–8 present time series of simulated concentrations of CO, PM₁₀ and O₃ in the Moscow region in comparison with corresponding monitoring data. Supplementary meteorological information is presented in Fig. 9. Simulations were performed both with and without fire emissions (see the curves for the FE and REF runs, respectively). Concentrations of primary pollutants used in our optimization procedure are presented separately for the two groups of sites (see Sect. 2.2), one of which is used for optimization of wildfire emissions and another – only for validation of model results. Note that CO and PM₁₀ concentrations are shown with a logarithmic scale.

The observed CO and PM₁₀ concentrations exhibited very strong positive perturbations in the period from 3 to 15 August. The largest CO and PM₁₀ concentrations were observed in Moscow on 7 August (68th day at the figures). Specifically, average (over all of the monitors considered in this study) concentrations of CO and PM₁₀ exceeded 10 mg m^{-3} and $700 \text{ } \mu\text{g m}^{-3}$, respectively, while the maximum daily mean concentrations registered at individual monitoring sites in Moscow in that day reached 20 mg m^{-3} for CO and $900 \text{ } \mu\text{g m}^{-3}$ for PM₁₀. These concentrations significantly exceeded threshold values established by Russian air quality standards (which are 3 mg m^{-3} and 150

Atmospheric impacts of the 2010 Russian wildfires

I. B. Konovalov et al.

Title Page

Abstract

Introduction

Conclusions

References

Tables

Figures

◀

▶

◀

▶

Back

Close

Full Screen / Esc

Printer-friendly Version

Interactive Discussion



$\mu\text{g m}^{-3}$ for daily mean of CO and PM₁₀ concentrations, respectively). Very large aerosol concentrations were associated with strongly reduced visibility (see Fig. 10). The observed ozone concentrations were also enhanced in August, but to a lesser extent than primary pollutant concentrations. Interestingly, the peaks of CO and PM₁₀ concentrations on 7 August were not associated with a similar maximum in ozone. In general, temporal variability in the ozone time series is much larger than that for CO and PM₁₀, reflecting a more complex nature of the ozone evolution.

The formation of the strong air pollution episodes took place in the hot and dry atmosphere inside of a blocking anticyclone accumulating tropical air transported to Western Russia from south. Maximum daily temperature mostly exceeded 30 °C in July and August (see Fig. 9), surpassing record values registered at the same site over a period of more than 100 years, and there was almost no precipitation in July and in the beginning of August.

Simulations taking into account wildfire emissions reproduce the CO and PM₁₀ observations fairly well. Specifically, the correlation coefficient calculated for the daily time series exceeds 0.8 both for CO and PM₁₀ and for all of the data subsets. Importantly, inclusion of fire emissions in the model leads to drastic improvements in agreement between the observed and simulated data. In particular, the root mean square error (RMSE) calculated for the validation subset of CO concentrations is reduced by more than 45% and the correlation coefficient increased from 0.41 to 0.86. Although the reduction of RMSE is smaller for the validation subset of PM₁₀ concentrations (only about 10%), the increase of the correlation coefficient is also quite impressive: from 0.5 to 0.87. The reduction of RMSE for the optimisation subset of PM₁₀ data is also large (about 50%). The differences in results obtained with optimisation and validation subsets of PM₁₀ data may be due to a considerable representativity error in our PM₁₀ simulations which cannot be sufficiently reduced by averaging of PM₁₀ concentrations over a few measurement sites.

Ozone simulations also improve after taking fire emissions into account, but to a smaller extent. Specifically, the correlation coefficient increases from 0.61 to 0.74 and

Atmospheric impacts of the 2010 Russian wildfires

I. B. Konovalov et al.

Title Page

Abstract

Introduction

Conclusions

References

Tables

Figures



Back

Close

Full Screen / Esc

Printer-friendly Version

Interactive Discussion



RMSE decreases from 76 to $65 \mu\text{g m}^{-3}$. Not so good performance of ozone simulations may reflect strong temporal and spatial variability of ozone concentrations in the megacity region, especially in the presence of large perturbations of atmospheric composition due to fires. Some factors affecting the ozone behaviour are examined in Sect. 5.3.

Contribution of fires to air pollution in the Moscow region can be assessed as the difference between simulations performed with and without fire emissions. Evidently, the extreme air pollution episode in August was mainly caused by fires. Although stagnant meteorological conditions and high temperature which dominated in the Moscow region during July and August (see Fig. 9) favoured accumulation of primary pollutants and formation of secondary aerosols, our simulations in the REF case demonstrate that if wildfires would have been absent, the evolution of CO and PM_{10} concentrations would not have demonstrated any dramatic anomalies. On the other hand, the large impact of fires on air quality in Moscow was favoured by specific circulations patterns: additional analysis (not presented here) of the spatial-temporal evolution of the simulated concentration fields reveals that the air pollution episode in Moscow in the period from 3 to 15 August was mainly caused by transport of smoke from intensive fires north to Ryazan (the city situated in ~ 180 km south-east from Moscow). As an illustration, Fig. 11 presents the HYSPLIT (<http://ready.arl.noaa.gov/hysplit-bin>) backward trajectory analysis for 7 August, which confirms that the air transport to Moscow took place from the south-west direction, among other directions.

Ozone can be affected by wild fires at least in two different ways. On the one hand, wildfire emissions favor photochemical ozone formation by increasing ozone precursor levels (NO_x , VOC, CO). On the other hand, smoke aerosol absorbs solar radiations and thus inhibits ozone formation. The reference (REF) simulation presented in Fig. 8 was performed without fire emissions, but the impact of fires on photolytic reactions was still included (via the observational constraint as discussed above). In this case, unlike CO and PM_{10} , ozone could still reach rather high values ($>300 \mu\text{g m}^{-3}$). At the same time, the base case (FE) run yields much higher ozone concentrations than the

Atmospheric impacts of the 2010 Russian wildfires

I. B. Konovalov et al.

Title Page

Abstract

Introduction

Conclusions

References

Tables

Figures

◀

▶

◀

▶

Back

Close

Full Screen / Esc

Printer-friendly Version

Interactive Discussion



REF run in two episodes (26–29 July and 4–11 August), clearly showing the impact of fire emissions. The impact of the shielding effect of aerosol on the ozone evolution is assessed in Sect. 5.3.

5.3 Sensitivity tests

In this section, we present results of several numerical experiments clarifying the role of different factors in the considered phenomena. First, we tried to better understand the origin of the extreme air pollution episodes in Moscow. For this purpose, we examined whether these episodes were caused by relatively local fires or were due to transport of air pollution from more distant regions. Specifically, we performed a test simulation (TEST_1) where wildfire emissions in a small region surrounding Moscow were put to zero. The region boundaries were defined as follows: 37° E, 41° E, 54.5° N and 56° N, i.e. less than 200 km from Moscow. This region includes, in particular, locations of intensive fires near Ryazan (see Fig. 5f and h). Results presented in Fig. 12 unambiguously confirm that the extreme air pollution episodes in Moscow were caused by fires taking place at relatively short range from Moscow, although the impact of more distant fires is also not negligible, especially in the period from 7 to 11 August.

The goal of the next experiment is to justify the importance of the parameter $C(\tau)$, which is expected to compensate for a possible underestimation of FRP from fires obscured by smoke aerosols. In the case of $C(\tau) = 1$, the optimization procedure described in Sect. 4.2 yielded the following values of the correction factors for CO fire emissions: $F_1 = 0.93$ and $F_2 = -1.3$. Negative values of emissions from peat fires are physically unacceptable, and this result is evidence that if the impact of smoke aerosols on the FRP measurements is disregarded, the emission model defined by Eq. (6) becomes inadequate. With F_2 fixed at zero, we found that the optimal value of F_1 is 0.88. The corresponding CO concentrations are presented in Fig. 13. Evidently, the performance of the simulations is much worse in the test case than in the base case. Therefore, this test justifies the proposed parameterization of $C(\tau)$, even though we cannot claim that it is the best possible.

Atmospheric impacts of the 2010 Russian wildfires

I. B. Konovalov et al.

Title Page

Abstract

Introduction

Conclusions

References

Tables

Figures

◀

▶

◀

▶

Back

Close

Full Screen / Esc

Printer-friendly Version

Interactive Discussion



**Atmospheric impacts
of the 2010 Russian
wildfires**

I. B. Konovalov et al.

[Title Page](#)[Abstract](#)[Introduction](#)[Conclusions](#)[References](#)[Tables](#)[Figures](#)[⏪](#)[⏩](#)[◀](#)[▶](#)[Back](#)[Close](#)[Full Screen / Esc](#)[Printer-friendly Version](#)[Interactive Discussion](#)

The next experiments examine the impact of the shielding effect of smoke aerosols on the evolution of surface ozone in the Moscow region. Simulations were performed for the TEST_3 and TEST_4 cases which were the same as the reference (REF) and base (FE) cases discussed above (that is, without and with fire emissions), respectively, except that the effect of aerosol on photolysis rates was disregarded. The results presented in Fig. 14 indicate that even if fires were absent, ozone concentration in the Moscow region under very hot, stagnant and cloudless conditions of August 2010 could reach very high values. Comparison of results of the tests with the base case (FE) simulations confirms that wildfires strongly affected ozone formation in the two ways, namely by providing a powerful source of ozone precursors and, at the same time, inhibiting its formations as a result of absorption of solar radiation by smoke aerosols. The net result of these two effects was different in different conditions.

The purpose of a final test is to assess ozone sensitivity to heterogeneous reactions specified in the standard version of CHIMERE. Figure 15 presents the ozone evolution simulated as in the FE case but taking into account the standard set (see Sect. 3.1) of heterogeneous reactions (the TEST_5 case) in comparison with ozone time series obtained in the FE case. Evidently, the impact of heterogeneous reactions on ozone concentrations is small except for one day (7 August) associated with largest concentrations of smoke aerosols. Our results show that during this day, heterogeneous reactions substantially increased ozone production, probably mainly through the Reaction (R3) providing an additional source of odd hydrogen through heterogeneous HONO formation and subsequent photolysis. However, accounting for heterogeneous reactions did not lead to improving of model performance statistics. Therefore, our results indicate that further research is needed to examine the role of atmospheric heterogeneous processes under heavy smoke conditions in the evolution of atmospheric composition.

5.4 Air pollution episodes in the Moscow megacity region from a continental scale perspective: comparison of model results with MOPITT CO measurements

The severe air pollution episodes observed in the Moscow region were only a part of a strong perturbation in the atmospheric composition caused by wildfires in Russia. To understand the spatial extent of these perturbations and to evaluate the representativity of phenomena observed in Moscow within a more general picture, it is useful to consider modeling results together with satellite measurements.

Figure 16 presents a daily time series of the CO mixing ratio at 900 hPa, derived from MOPITT measurements in comparison with a corresponding time series of the simulated data. All data were spatially averaged over the whole European model domain. According to the measurements, the period from about 3 August to 17 August was associated with a strong perturbation of the spatially average CO mixing ratio. The model systematically underestimates the measurements (the average bias is about 16 ppb), and the day-to-day variability is smaller in simulations than in measurements. Nonetheless, it is important that inclusion of fire emissions into our model improves the agreement between the simulated and measured variation of CO mixing ratios at the continental scale.

When discussing systematic differences between the measured and modeled CO mixing ratio, it should be considered that 900 hPa MOPITT measurements are actually sensitive to CO over the whole troposphere, as explained in Sect. 3.2. For instance, the mean (over the whole model domain and the summer season 2010) sensitivity to CO at 500 hPa is still as large as that at 900 hPa. Pfister et al. (2004) detected an even larger positive systematic difference than in our study (up to 30 ppb in summer) between CO mixing ratios from MOPITT and the MOZART global CTM and found that only 8% of CO at 500 hPa over Europe originated from European emissions. Accordingly, one probable reason for the bias detected in this study is a systematic underestimation of monthly average climatological CO lateral and top boundary conditions that are indeed taken

Atmospheric impacts of the 2010 Russian wildfires

I. B. Konovalov et al.

Title Page

Abstract

Introduction

Conclusions

References

Tables

Figures



Back

Close

Full Screen / Esc

Printer-friendly Version

Interactive Discussion



from MOZART. Pfister et al. (2004) also argue that a significant part of the mentioned difference is due to an underestimation of anthropogenic CO emissions in their model. Thus, both CO emissions, but also advection through model boundaries, are potential error sources. Taking into account that the modeled CO concentrations are not inconsistent with ground based measurements, the underestimation of fire emissions seems to be a less probable reason, although the optimized emissions may indeed be lower than in reality if a part of pyrogenic CO was injected directly into the free troposphere.

The comparison of spatial distributions of the measured and modeled CO mixing ratio is presented in Fig. 17. MOPITT measurements show that the CO level was strongly enhanced over most of the European part of Russia. The huge CO “cloud” also covered parts of Belarus and Ukraine. The model reproduces the location of the maximum CO mixing ratio perturbation in the south-east of Moscow reasonably well, but underestimates its magnitude even after correction of the systematic bias. It appears that the CO distribution from the model is much smoother than that from MOPITT. The model also underestimates the CO mixing ratios in the southern part of the domain. In spite of certain differences with the satellite measurements, the simulations confirm the role of fires as the principal reason for the extreme air pollution observed over Russia in August 2010.

6 Conclusions

The CHIMERE chemistry transport model in combination with data of satellite and ground based measurements was used in order to analyze episodes of extreme air pollution in the Moscow megacity region in summer 2010, when maximum measured daily average CO and PM₁₀ concentrations reached 20 mg m⁻³ and 0.9 mg m⁻³, respectively. The model was modified by taking into account wildfire emissions and reduction of photolysis rates due to the shielding effect of aerosols. The wildfire emission estimates derived from the MODIS FRP measurements were optimized by assimilating data of air pollution monitoring in Moscow into the model. Specifically, we optimized

Atmospheric impacts of the 2010 Russian wildfires

I. B. Konovalov et al.

Title Page

Abstract

Introduction

Conclusions

References

Tables

Figures

◀

▶

◀

▶

Back

Close

Full Screen / Esc

Printer-friendly Version

Interactive Discussion



two factors relating FRP data to rates of wildfire emissions separately from peat land and other types of land cover. In this way, we managed to estimate both total wildfire emissions and emissions from peat fires. The impact of smoke aerosols on photolysis rates was taken into account in a simplified way using the aerosol optical depth (AOD) measured by MODIS at 550 nm. The MODIS AOD measurements were used also to compensate for a possible negative bias in FRP measurements in case of fires obscured by heavy smoke.

Validation of the model results was performed by comparing them with independent monitoring data which were withheld during the optimisation procedure. It is demonstrated that the optimized simulations reproduce PM_{10} , CO, and O_3 monitoring data rather adequately. Specifically, the correlation coefficient of daily time series of CO and PM_{10} exceeds 0.85 and is equal to 0.74 in the case of the times series of ozone daily maximums. It is also found that inclusion of fire emissions into the model significantly improves its performance. In particular, the correlation coefficient calculated for daily CO concentrations in the validation data subset has increased from 0.41 up to 0.86, and RMSE has been reduced from 1.53 to 0.81 $mg\ m^{-3}$. Therefore, this study confirmed the feasibility of using satellite measurements of the fire radiative power for estimation of emissions of air pollutants from wildfires.

The comparison of model results obtained without and with fire emissions showed that wildfires were a principal factor causing observed episodes of extremely high concentrations of CO and PM_{10} in the Moscow region. Accumulation of anthropogenic pollution favoured by stagnant and dry meteorological conditions could also lead to exceeding of air quality standards in Moscow, but anthropogenic sources of primary air pollutants could not compete with the huge wildfire emissions. Although the measured ozone concentration, similar to concentrations of CO and PM_{10} , were strongly elevated during the considered period, our diagnostic simulations revealed that it could be very large even without fire emissions which provide a powerful source of ozone precursors but, at the same time, inhibit its formations as a result of absorption of solar radiation by smoke aerosols.

Atmospheric impacts of the 2010 Russian wildfires

I. B. Konovalov et al.

[Title Page](#)[Abstract](#)[Introduction](#)[Conclusions](#)[References](#)[Tables](#)[Figures](#)[⏪](#)[⏩](#)[◀](#)[▶](#)[Back](#)[Close](#)[Full Screen / Esc](#)[Printer-friendly Version](#)[Interactive Discussion](#)

**Atmospheric impacts
of the 2010 Russian
wildfires**I. B. Konovalov et al.

[Title Page](#)[Abstract](#)[Introduction](#)[Conclusions](#)[References](#)[Tables](#)[Figures](#)[⏪](#)[⏩](#)[◀](#)[▶](#)[Back](#)[Close](#)[Full Screen / Esc](#)[Printer-friendly Version](#)[Interactive Discussion](#)

Additional numerical experiments aimed at clarifying the role of different factors in the considered phenomena. In particular, the extreme air pollution episodes in Moscow were mainly caused by fires taking place at relatively short range (less than 200 km) from Moscow; the transport of air pollution to Moscow from more distant (although also intensive) fires was less significant. It was also found that a compensation of a possible negative bias in the measured radiative power from fires obscured by heavy smoke is a crucial condition for a good performance of the model.

The MOPITT CO measurements and corresponding simulations indicate that the observed episodes of extreme air pollution in Moscow were only a part of a very strong perturbation of the atmospheric composition, caused by wildfires, over the largest part of European Russia. Wildfire emission estimates consistent with the measurements in the Moscow region suggest that fires in Western Russia emitted more than 85% (~9.7 Tg) of the total annual anthropogenic CO emissions in the same region. On the whole, this study demonstrated that wildfires can play a crucial role for air pollution even in large megacity regions otherwise strongly affected by anthropogenic air pollution. Efforts to properly address atmospheric effects associated with wildfires in chemistry transport models should be continued in future studies. In particular, heterogeneous reactions occurring on fire emitted aerosols should be included into the model.

Acknowledgements. The support for this study was provided by the Russian Foundation for Basic Research (grants No. 11-05-91061-CNRS, 11-05-97003-r), Russian Academy of Sciences in the framework of the Programme for Basic Research “Electrodynamics of atmosphere; Electrical Processes, Radiophysical Methods of Research”, Russian Federal Special Program “Scientific and scientifically-pedagogical staff of innovative Russia” in 2009–2013 (contracts 02.740.11.0732, P2318) and the Government of the Russian Federation under the agreement No. 11.G34.31.0014.

The publication of this article is financed by CNRS-INSU.

References

- 2010 Russian wildfires: Wikipedia, The Free Encyclopedia, <http://en.wikipedia.org> (last access: February 2011), 2011.
- 5 Akagi, S. K., Yokelson, R. J., Wiedinmyer, C., Alvarado, M. J., Reid, J. S., Karl, T., Crouse, J. D., and Wennberg, P. O.: Emission factors for open and domestic biomass burning for use in atmospheric models, *Atmos. Chem. Phys. Discuss.*, 10, 27523–27602, doi:10.5194/acpd-10-27523-2010, 2010.
- 10 Andreae, M. O. and Merlet, P.: Emission of trace gases and aerosols from biomass burning, *Global Biogeochem. Cy.*, 15, 955–966, 2001.
- Aumont, B., Chervier, F., and Laval, S.: Contribution of HONO to the NO_x/HO_x/O₃ chemistry in the polluted boundary layer, *Atmos. Environ.*, 37, 487–498, 2003.
- Barbu, A. L., Segers, A. J., Schaap, M., Heemink, A. W., and Builtjes, P. J. H.: A multi-component data assimilation experiment directed to sulphur dioxide and sulphate over Europe, *Atmos. Environ.*, 43(9), 1622–1631, doi:10.1016/j.atmosenv.2008.12.005, 2009.
- 15 Beekmann, M. and Vautard, R.: A modelling study of photochemical regimes over Europe: robustness and variability, *Atmos. Chem. Phys.*, 10, 10067–10084, doi:10.5194/acp-10-10067-2010, 2010.
- 20 Bessagnet, B., Menut, L., Aymoz, G., Chepfer, H., and Vautard, R.: Modelling dust emissions and transport within Europe: the Ukraine March 2007 event, *J. Geophys. Res.-Atmos.*, 113, D15202, doi:10.1029/2007JD009541, 2008.
- Christian, T. J., Kleiss, B., Yokelson, R. J., Holzinger, R., Crutzen, P. J., Hao, W. M., Sahaarjo, B. H., and Ward, D. E.: Comprehensive laboratory measurements of biomass-burning

Atmospheric impacts of the 2010 Russian wildfires

I. B. Konovalov et al.

Title Page

Abstract

Introduction

Conclusions

References

Tables

Figures

⏪

⏩

◀

▶

Back

Close

Full Screen / Esc

Printer-friendly Version

Interactive Discussion



Atmospheric impacts of the 2010 Russian wildfires

I. B. Konovalov et al.

Title Page

Abstract

Introduction

Conclusions

References

Tables

Figures

◀

▶

◀

▶

Back

Close

Full Screen / Esc

Printer-friendly Version

Interactive Discussion



- emissions: 1. Emissions from Indonesian, African, and other fuels, *J. Geophys. Res.*, 108(D23), 4719, doi:10.1029/2003JD003704, 2003.
- Crutzen, P. J. and Andreae, M. O.: Biomass burning in the tropics: Impact on atmospheric chemistry and biogeochemical cycles, *Science*, 250, 1669–1678, 1990.
- 5 Deeter, M. N. and MOPITT algorithm development team: MOPITT (Measurements of Pollution in the Troposphere) validated version 4 product user's guide, NCAR, Boulder, 2009.
- Dickerson, R. R., Kondragunta, S., Stenchikov, G., Civerolo, K. L., Doddridge, B. G., and Holben, B. N.: The impact of aerosols on solar ultraviolet radiation and photochemical smog, *Science*, 278, 827–830, 1997.
- 10 Elbern, H., Strunk, A., Schmidt, H., and Talagrand, O.: Emission rate and chemical state estimation by 4-dimensional variational inversion, *Atmos. Chem. Phys.*, 7, 3749–3769, doi:10.5194/acp-7-3749-2007, 2007.
- EMEP: Transboundary acidification, eutrophication and ground level ozone in Europe in 2008, Joint MSC-W & CCC & CEIP Report, EMEP Status Report 1/10, 2010.
- 15 Enting, I. G.: Inverse problems in atmospheric constituents transport, Cambridge University Press, 2002.
- Eskes, H. J., Piters, A. J. M., Levelt, P. F., Allart, M. A. F., and Kelder, H. M.: Variational assimilation of total-column ozone satellite data in a 2D lat-lon tracer-transport model, *J. Atmos. Sci.*, 56, 3560–3572, 1999.
- 20 Giglio, L., Descloitres, J., Justice, C. O., and Kaufman, Y. J.: An enhanced contextual fire detection algorithm for MODIS, *Remote. Sens. Environ.*, 87, 273–282, doi:10.1016/S0034-4257(03)00184-6, 2003.
- Giglio, L., van der Werf, G. R., Randerson, J. T., Collatz, G. J., and Kasibhatla, P.: Global estimation of burned area using MODIS active fire observations, *Atmos. Chem. Phys.*, 6, 957–974, doi:10.5194/acp-6-957-2006, 2006.
- 25 Giglio, L.: MODIS Collection 5 Active Fire Product User's Guide, Science Systems and Applications, Inc., University of Maryland, 2010.
- Ginoux, P., Chin, M., Tegen, I., Prospero, J. M., Holben, B., Dubovik, O., and Lin, S.-J.: Sources and distributions of dust aerosols simulated with the GOCART model, *J. Geophys. Res.*, 106, 20255–20273, 2001.
- 30 Gorchakov, G. I., Semutnikova, E. G., Zotkin, E. V., Karpov, A. V., Lezina, E. A., and Ul'yanenko, A. V.: Variations in Gaseous Pollutants in the Air Basin of Moscow, *Izvestiya, Atmos. Ocean. Phys.*, 42(2), 156–170, 2006.

- GPW: Global Population of the World, version 3, SEDAC, <http://sedac.ciesin.columbia.edu/gpw> (last access: February 2011), 2010.
- Grégoire, J. M., Tansey, K., and Silva, J. M. N.: The GBA2000 initiative: developing a global burnt area database from SPOTVEGETATION imagery, *Int. J. Remote. Sens.*, 24, 1369–1376, doi:10.1080/0143116021000044850, 2003.
- Hao, W. M., Ward, D. E., Olbu, G., and Baker, S. P.: Emissions of CO₂, CO, and hydrocarbons from fires in diverse African savanna ecosystems, *J. Geophys. Res.-Atmos.*, 101, 23577–23584, 1996.
- Harrison, R. and Kito, A.: Field intercomparison of filter pack and denuder sampling methods for reactive gaseous and particulate pollutants, *Atmos. Environ.*, 24, 2633–2640, 1990.
- Hodzic, A., Vautard, R., Bessagnet, B., Lattuati, M., and Moreto, F.: Long-term urban aerosol simulation versus routine particulate matter observations, *Atmos. Environ.*, 39, 5851–5864, 2005.
- Hodzic, A., Madronich, S., Bohn, B., Massie, S., Menut, L., and Wiedinmyer, C.: Wildfire particulate matter in Europe during summer 2003: meso-scale modeling of smoke emissions, transport and radiative effects, *Atmos. Chem. Phys.*, 7, 4043–4064, doi:10.5194/acp-7-4043-2007, 2007.
- Horowitz, L. W., Walters, S., Mauzerall, D. L., Emmons, L. K., Rasch, P. J., Granier, C., Tie, X., Lamarque, J.-F., Schultz, M. G., Tyndall, G. S., Orlando, J. J., and Brasseur, G. P.: A global simulation of ozone and related tracers: description and evaluation of MOZART, Version 2, *J. Geophys. Res.*, 108(D24), 4784, doi:10.1029/2002JD002853, 2003.
- Ichoku, C. and Kaufman, J. Y.: A Method to Derive Smoke Emission Rates From MODIS Fire Radiative Energy Measurements, *IEEE T. Geosci. Remote*, 43(11), 2636–2649, 2005.
- Ichoku, C., Remer, L. A., and Eck, T. F.: Quantitative evaluation and intercomparison of morning and afternoon Moderate Resolution Imaging Spectroradiometer (MODIS) aerosol measurements from Terra and Aqua, *J. Geophys. Res.*, 110, D10S03, doi:10.1029/2004JD004987, 2005.
- Iinuma, Y., Brüggemann, E., Gnauk, T., Müller, K., Andreae, M. O., Helas, G., Parmar, R., and Herrmann, H.: Source characterization of biomass burning particles: The combustion of selected European conifers, African hardwood, savanna grass, and German and Indonesian peat, *J. Geophys. Res.*, 112, D08209, doi:10.1029/2006JD007120, 2007.
- Jacob, D. J.: Heterogeneous chemistry and tropospheric ozone, *Atmos. Environ.*, 34(34), 2131–2159, 2000.

**Atmospheric impacts
of the 2010 Russian
wildfires**

I. B. Konovalov et al.

Title Page

Abstract

Introduction

Conclusions

References

Tables

Figures

◀

▶

◀

▶

Back

Close

Full Screen / Esc

Printer-friendly Version

Interactive Discussion



**Atmospheric impacts
of the 2010 Russian
wildfires**

I. B. Konovalov et al.

Title Page

Abstract

Introduction

Conclusions

References

Tables

Figures

◀

▶

◀

▶

Back

Close

Full Screen / Esc

Printer-friendly Version

Interactive Discussion



- Jaffe, D., Bertschi, I., Jaegle, L., Novelli, P., Reid, J. S., Tanimoto, H., Vingarzan, R., and Westphal, D. L.: Long-range transport of Siberian biomass burning emissions and impact on surface ozone in western North America, *Geophys. Res. Lett.*, 31, L16106, doi:10.1029/2004GL020093, 2004.
- 5 Jain, A. K., Tao, Z. N., Yang, X. J., and Gillespie, C.: Estimates of global biomass burning emissions for reactive greenhouse gases (CO, NMHCs, and NO_x) and CO₂, *J. Geophys. Res.-Atmos.*, 111, D06304, doi:10.1029/2005JD006237, 2006.
- Jeong, J. I., Park, R. J., and Youn, D.: Effects of Siberian forest fires on air quality in East Asia during May 2003 and its climate implication, *Atmos. Environ.*, 42, 8910–8922, doi:10.1016/j.atmosenv.2008.08.037, 2008.
- 10 Kaiser, J. W., Suttie, M., Flemming, J., Morcrette, J.-J., Boucher, O., and Schultz, M. G.: Global Real-time Fire Emission Estimates Based on Space-borne Fire Radiative Power Observations, CP1100, in: *Current Problems in Atmospheric Radiation (IRS 2008)* edited by: Nakajima, T. and Yamasoe, M. A., American Institute of Physics, NY, 645–648, 2009.
- 15 Kaufmann, Y. J., Tanre, D., Remer, L. A., Vermote, E. F., Chu, A., and Holben, B. N.: Operational remote sensing of tropospheric aerosol over land from EOS moderate resolution imaging spectroradiometer, *J. Geophys. Res.*, 102(D14), 17051–17 067, 1997.
- Kaufman, Y. J., Justice, C. O., Flynn, L. P., Kendall, J. D., Prins, E. M., Giglio, L., Ward, D. E., Menzel, W. P., and Setzer, A. W.: Potential global fire monitoring from EOS-MODIS, *J. Geophys. Res.*, 103, 32215–32238, 1998.
- 20 Key, J.: *Streamer User's Guide*, Cooperative Institute for Meteorological Satellite Studies, University of Wisconsin, 96 pp., 2001.
- Konovalov, I. B., Beekmann, M., Vautard, R., Burrows, J. P., Richter, A., Nüß, H., and Elansky, N.: Comparison and evaluation of modelled and GOME measurement derived tropospheric NO₂ columns over Western and Eastern Europe, *Atmos. Chem. Phys.*, 5, 169–190, doi:10.5194/acp-5-169-2005, 2005.
- 25 Konovalov, I. B., Beekmann, M., Burrows, J. P., and Richter, A.: Satellite measurement based estimates of decadal changes in European nitrogen oxides emissions, *Atmos. Chem. Phys.*, 8, 2623–2641, doi:10.5194/acp-8-2623-2008, 2008.
- 30 Konovalov, I. B., Elanskii, N. F., Zvyagintsev, A. M., Belikov, I. B., and Beekmann, M.: Validation of chemistry transport model of the lower atmosphere in the Central European region of Russia using ground-based and satellite measurement data, *Russ. Meteorol. Hydrol.*, 34(4), 236–242, 2009.

**Atmospheric impacts
of the 2010 Russian
wildfires**

I. B. Konovalov et al.

Title Page

Abstract

Introduction

Conclusions

References

Tables

Figures

◀

▶

◀

▶

Back

Close

Full Screen / Esc

Printer-friendly Version

Interactive Discussion



Konovalov, I. B., Beekmann, M., Richter, A., Burrows, J. P., and Hilboll, A.: Multi-annual changes of NO_x emissions in megacity regions: nonlinear trend analysis of satellite measurement based estimates, *Atmos. Chem. Phys.*, 10, 8481–8498, doi:10.5194/acp-10-8481-2010, 2010.

5 Kuznetsova, I. N., Zaripov, R. B., Konovalov, I. B., Zvyagintsev, A. M., Semutnikova, E. G., and Artamonova, A. A.: The computational complex including a mesoscale atmospheric model and a chemistry transport model as a module of the air quality assessment system, *Atmos. Ocean. Opt.*, 23(06), 485–492, 2010.

10 Kuznetsova, I. N., Konovalov, I. B., Artamonova, A. A., Nakhaev, M. I., Lezina, E. A., Zvyagintsev, A. M., Beekmann, M.: The observed and simulated variability of PM_{10} concentration in Moscow and Zelenograd, *Russ. Meteorol. Hydrol.*, 36(3), 175–184, doi:10.3103/S1068373911030046, 2011.

Langmann, B., Duncan, B., Textor, C., Trentmann, J., and van der Werf, G. R.: Vegetation fire emissions and their impact on air pollution and climate, *Atmos. Environ.*, 43 107–116, doi:10.1016/j.atmosenv.2008.09.047, 2009.

15 Larkin, N. K., O'Neill, S. M., Solomon, R., Raffuse, S., Strand, T., Sullivan, D. C., Krull, C., Rorig, M., Peterson, J. L., and Ferguson, S. A.: The BlueSky smoke modeling framework, *Int. J. Wildland Fire*, 18, 906–920, 2009.

20 Lattuati, M.: Contribution à l'étude du bilan de l'ozone troposphérique à l'interface de l'Europe et de l'Atlantique Nord: Modélisation lagrangienne et mesures en altitude, Ph.D. Thesis, Université Paris 6, Paris, 1997.

Madronich, S., McKenzie, R. E., Bjorn, L. O., and Caldwell, M. M.: Changes in biologically active ultraviolet radiation reaching the earth's surface, *J. Photochem. Photobiol. B*, 46, 5–19, 1998.

25 Martin, R. V., Jacob, D. J., Yantosca, R. M., Chin, M., and Ginoux, P.: Global and regional decreases in tropospheric oxidants from photochemical effects of aerosols, *J. Geophys. Res.*, 108(D3), 4097, doi:10.1029/2002JD002622, 2003.

Meloni, D., di Sarra, A., Pace, G., and Monteleone, F.: Aerosol optical properties at Lampedusa (Central Mediterranean), 2. Determination of single scattering albedo at two wavelengths for different aerosol types, *Atmos. Chem. Phys.*, 6, 715–727, doi:10.5194/acp-6-715-2006, 2006.

Atmospheric impacts of the 2010 Russian wildfires

I. B. Konovalov et al.

Title Page

Abstract

Introduction

Conclusions

References

Tables

Figures

◀

▶

◀

▶

Back

Close

Full Screen / Esc

Printer-friendly Version

Interactive Discussion



Menut L., Chiapello, I., and Moulin, C.: Previsibility of mineral dust concentrations: The CHIMERE-DUST forecast during the first AMMA experiment dry season, *J. Geophys. Res.-Atmos.*, 114, D07202, doi:10.1029/2008JD010523, 2009.

Molina, M. J. and Molina, L. T.: Megacities and atmospheric pollution, *J. Air Waste Manage. Assoc.*, 54, 644–680, 2004.

Monge, M. E., D'Anna, B., Mazri, L., Giroir-Fendler, A., Ammann, M., Donaldson, D. J., and George, C.: Light changes the atmospheric reactivity of soot, *P. Natl. Acad. Sci.*, 107(15), 6605–6609, doi:10.1073/pnas.0908341107, 2010.

Muraleedharan, T. R., Radojevic, M., Waugh, A., and Caruana, A.: Emissions from the combustion of peat: an experimental study, *Atmos. Environ.*, 34, 3033–3035, 2000.

Park, R. J., Jacob, D. J., Chin, M., and Martin, R. V.: Sources of carbonaceous aerosols over the United States and implications for natural visibility, *J. Geophys. Res.*, 108(D12), 4355, doi:10.1029/2002JD003190, 2003.

Pfister, G., Pétron, G., Emmons, L. K., Gille, J. C., Edwards, D. P., Lamarque, J.-F., Attie, J.-L., Granier, C., and Novelli, P. C.: Evaluation of CO simulations and the analysis of the CO budget for Europe, *J. Geophys. Res.*, 109, D19304, doi:10.1029/2004JD004691, 2004.

Pfister, G., Hess, P. G., Emmons, L. K., Lamarque, J.-F., Wiedinmyer, C., Edwards, D. P., Pétron, G., Gille, J. C., and Sachse, G. W.: Quantifying CO emissions from the 2004 Alaskan wildfires using MOPITT CO data, *Geophys. Res. Lett.*, 32, L11809, doi:10.1029/2005GL022995, 2005.

Pfister, G. G., Wiedinmyer, C., and Emmons, L. K.: Impacts of the fall 2007 California wildfires on surface ozone: Integrating local observations with global model simulations, *Geophys. Res. Lett.*, 35, L19814, doi:10.1029/2008GL034747, 2008.

Press, W. H., Teukolsky, S. A., Vetterling, W. T., and Flannery, B. P.: *Numerical Recipes*, 2nd edition, Cambridge University Press, 1992.

Rouil, L., Honore, C., Vautard, R., Beekmann, M., Bessagnet, B., Malherbe, L., Meleux, F., Dufour, A., Elichegaray, C., Flaud, J.-M., Menut, L., Martin, D., Peuch, A., Peuch, V.-H., and Poisson, N., PREV'AIR : an operational forecasting and mapping system for air quality in Europe, *B. Am. Meteorol. Soc.*, 90, 73-83, doi:10.1175/2008BAMS2390.1, 2009.

Schmidt, H. C., Derognat, C., Vautard, R., and Beekmann, M.: A comparison of simulated and observed ozone mixing ratios for the summer of 1998 in western Europe, *Atmos. Environ.*, 35, 6277–6297, 2001.

- Seiler, W. and Crutzen, P. J.: Estimates of gross and net fluxes of carbon between the biosphere and atmosphere from biomass burning, *Climatic Change*, 2, 207–247, 1980.
- Sofiev, M., Vankevich, R., Lotjonen, M., Prank, M., Petukhov, V., Ermakova, T., Koskinen, J., and Kukkonen, J.: An operational system for the assimilation of the satellite information on wild-land fires for the needs of air quality modelling and forecasting, *Atmos. Chem. Phys.*, 9, 6833–6847, doi:10.5194/acp-9-6833-2009, 2009.
- Stavrakou, T., Müller, J.-F., De Smedt, I., Van Roozendaal, M., van der Werf, G. R., Giglio, L., and Guenther, A.: Evaluating the performance of pyrogenic and biogenic emission inventories against one decade of space-based formaldehyde columns, *Atmos. Chem. Phys.*, 9, 1037–1060, doi:10.5194/acp-9-1037-2009, 2009.
- Tarantola, A.: *Inverse problem theory; methods for data fitting and model parameter estimation*, Elsevier, 1987.
- Turquety, S., Logan, J. A., Jacob, D. J., Hudman, R. C., Leung, F. Y., Heald, C. L., Yantosca, R. M., Wu, S., Emmons, L. K., Edwards, D. P., and Sachse, G. W.: Inventory of boreal fire emissions for North America in 2004: the importance of peat burning and pyro-convective injection, *J. Geophys. Res.*, 112, D12S03, doi:10.1029/2006JD007281, 2007.
- Turquety, S., Hurtmans, D., Hadji-Lazaro, J., Coheur, P.-F., Clerbaux, C., Josset, D., and Tsamalis, C.: Tracking the emission and transport of pollution from wildfires using the IASI CO retrievals: analysis of the summer 2007 Greek fires, *Atmos. Chem. Phys.*, 9, 4897–4913, doi:10.5194/acp-9-4897-2009, 2009.
- UNECE: *Present state of emission data*, ECE/EB.AIR/97, 2009.
- Urbanski, S. P., Hao, W. M., and Baker, S.: *Chemical Composition of Wildland Fire Emissions*, in: *Developments in Environmental Science*, V. 8, edited by: Bytnerowicz, A., Arbaugh, M., Riebau, A., and Andersen, C., New York, Elsevier, 79–107, 2009.
- van der Werf, G. R., Randerson, J. T., Giglio, L., Collatz, G. J., Kasibhatla, P. S., and Arellano Jr., A. F.: Interannual variability in global biomass burning emissions from 1997 to 2004, *Atmos. Chem. Phys.*, 6, 3423–3441, doi:10.5194/acp-6-3423-2006, 2006.
- van der Werf, G. R., Randerson, J. T., Giglio, L., Collatz, G. J., Mu, M., Kasibhatla, P. S., Morton, D. C., DeFries, R. S., Jin, Y., and van Leeuwen, T. T.: Global fire emissions and the contribution of deforestation, savanna, forest, agricultural, and peat fires (1997-2009), *Atmos. Chem. Phys.*, 10, 11707–11735, doi:10.5194/acp-10-11707-2010, 2010.
- Vautard, R., Builtjes, P. H. J., Thunis, P., Cuvelier, C., Bedogni, M., Bessagnet, B., Honoré, C., Moussiopoulos, N., Pirovano, G., Schaap, M., Stern, R., Tarrason, L., and Wind, P.:

**Atmospheric impacts
of the 2010 Russian
wildfires**

I. B. Konovalov et al.

Title Page

Abstract

Introduction

Conclusions

References

Tables

Figures

◀

▶

◀

▶

Back

Close

Full Screen / Esc

Printer-friendly Version

Interactive Discussion



Atmospheric impacts of the 2010 Russian wildfires

I. B. Konovalov et al.

Title Page

Abstract

Introduction

Conclusions

References

Tables

Figures

◀

▶

◀

▶

Back

Close

Full Screen / Esc

Printer-friendly Version

Interactive Discussion



Evaluation and intercomparison of Ozone and PM₁₀ simulations by several chemistry transport models over four European cities within the CityDelta project, *Atmos. Environ.*, 41, 173–188, 2007.

Vestreng, V.: Inventory Review 2004, Emission data reported to CLRTAP and the NEC Directive, EMEP/EEA Joint Review report, EMEP/MSC-W Note 1, July, 2004.

Vompersky, S. J., Sirin, A. A., Cyganova, O. P., Valjaeva, N. A., and Majkov, D. A.: Bolota i zabolochennye zemli Rossii: popytka analiza prostranstvennogo raspredelenija i raznoobrazija, *Izvestiya RAN, Seriya Geograficheskaya*, 5, 39–50, 2005.

Wang, J., Christopher, S. A., Nair, U. S., Reid, J. S., Prins, E. M., Szykman, J., and Hand, J. L.: Mesoscale modeling of Central American smoke transport to the United States: 1. “Top-down” assessment of emission strength and diurnal variation impacts, *J. Geophys. Res.*, 111, D05S17, doi:10.1029/2005JD006416, 2006.

Wiedinmyer, C., Quayle, B., Geron, C., Belote, A., McKenzie, D., Zhang, X., O’Neill, S., and Wynne, K. K.: Estimating emissions from fires in North America for air quality modeling, *Atmos. Environ.*, 40, 3419–3432, doi:10.1016/j.atmosenv.2006.02.010, 2006.

Wooster, M. J., Zhukov, B., and Oertel D.: Fire radiative energy for quantitative study of biomass burning: Derivation from the BIRD experimental satellite and comparison to MODIS fire products, *Remote Sens. Environ.*, 86, 83–107, 2003.

Wooster, M. J., Roberts, G., Perry, G. L. W., and Kaufman, Y. J.: Retrieval of biomass combustion rates and totals from fire radiative power observations: FRP derivation and calibration relationships between biomass consumption and fire radiative energy release, *J. Geophys. Res.*, 110, D24311, doi:10.1029/2005JD006318, 2005.

WRAP – Western Regional Air Partnership: Development of 2000-04 Baseline Period and 2018 Projection Year Emission Inventories, Prepared by Air Sciences, Inc. Project No. 178-8, August, 2005.

Yokelson, R. J., Ward, D. E., Susott, R. A., Reardon, J., and Griffith, D. W. T.: Emissions from smoldering combustion of biomass measured by open-path Fourier transform infrared spectroscopy, *J. Geophys. Res.*, 102(D15), 18865–18877, 1997.

Zvyagintsev, A. M., Belikov, I. B., Egorov, V. I., Elansky, N. F., Kruchenitsky, G. M., Kuznetsova, I. N., Nikolaev, A. N., Obukhova, Z. V., and Skorokhod, A. I.: Positive anomalies in the surface ozone concentrations in July–August 2002 over Moscow and its suburbs *Izvestiya, Atmos. Ocean. Phys.*, 40(1), 68–79, 2004.

Atmospheric impacts of the 2010 Russian wildfires

I. B. Konovalov et al.

Title Page

Abstract

Introduction

Conclusions

References

Tables

Figures

◀

▶

◀

▶

Back

Close

Full Screen / Esc

Printer-friendly Version

Interactive Discussion



Table 1. Summary of settings of different model runs performed in the framework of this study.

Model run names (abbreviation)	Fire emissions	Aerosol impact on photolysis rates	Heterogeneous chemistry
REF	No	Yes	No
FE	Yes	Yes	No
TEST_1	Yes*	Yes	No
TEST_2	Yes**	Yes	No
TEST_3	No	No	No
TEST_4	Yes	No	No
TEST_5	Yes	Yes	Yes

*Wildfire emissions in a small region surrounding Moscow are put to zero, see Sect. 5.3 for details.

**Wildfire emissions are estimated without accounting for a possible attenuation of the measured FRP by smoke from fires ($C(\tau) = 1$, see Eq. 6).

Atmospheric impacts of the 2010 Russian wildfires

I. B. Konovalov et al.

Title Page

Abstract

Introduction

Conclusions

References

Tables

Figures

◀

▶

◀

▶

Back

Close

Full Screen / Esc

Printer-friendly Version

Interactive Discussion



Table 2. Biomass burning emission factors (g kg^{-1}) specified in the fire emission model (see Eq. 6) for different types of land. Note that the emission factors for four other surface types (bare land, inland water, ocean, and urban) considered in CHIMERE are set to be zero.

	agricultural	grass	shrubs	needleleaf forest	broadleaf forest	peatland
CO	70	90	84	8.9	94	210
NO _x (as NO)	2.4	6.5	3.2	2.5	2.1	1.0
NMHC	6.7	5.0	3.2	6.3	6.8	24.3
SO _x	0.4	0.5	0.5	0.8	0.8	0.5
NH ₃	1.5	0.6	0.6	0.9	0.6	14.3
PM _{2.5}	5.7	9.5	5.6	11.7	11.2	9.5
PM ₁₀	6.9	12.5	6.9	13.7	12.5	12.5

**Atmospheric impacts
of the 2010 Russian
wildfires**

I. B. Konovalov et al.

[Title Page](#)[Abstract](#)[Introduction](#)[Conclusions](#)[References](#)[Tables](#)[Figures](#)[⏪](#)[⏩](#)[◀](#)[▶](#)[Back](#)[Close](#)[Full Screen / Esc](#)[Printer-friendly Version](#)[Interactive Discussion](#)

Table 3. Optimal estimates of the correction factors F_1 and F_2 (see Eq. 6). The uncertainties reported in brackets are evaluated as the geometric standard deviation corresponding to the 68.3th percentile of the probability distributions of logarithms of the correction factors obtained in a Monte Carlo experiment.

	F_1	F_2
CO	0.24 (1.52)	1.68 (1.72)
PM	0.12 (1.25)	1.38 (1.61)

Atmospheric impacts of the 2010 Russian wildfires

I. B. Konovalov et al.

Title Page

Abstract

Introduction

Conclusions

References

Tables

Figures

⏪

⏩

◀

▶

Back

Close

Full Screen / Esc

Printer-friendly Version

Interactive Discussion



Table 4. Estimates of total amounts of CO (Tg) emitted in different regions and months in summer 2010.

	June		July		August	
	All fires	Peat fires	All fires	Peat fires	All fires	Peat fires
Central European Russia	<0.01	<0.01	1.33	0.42	4.89	1.58
European Russia	0.03	<0.01	1.83	0.57	7.85	2.60
Europe	0.14	<0.01	2.29	0.57	8.31	2.60

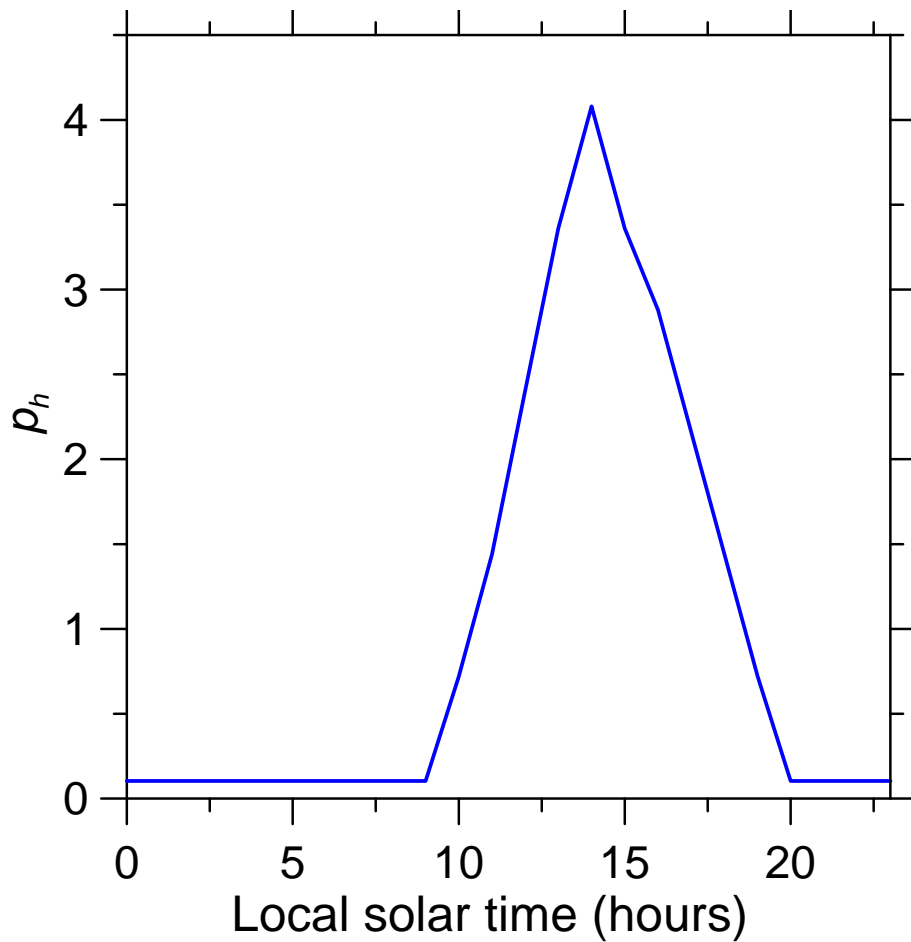


Fig. 1. The diurnal profile of emissions from wildfires, p_h (see Eq. 3), which is used to convert MODIS FRP measurements to hourly emissions of model species.

Atmospheric impacts of the 2010 Russian wildfires

I. B. Konovalov et al.

Title Page

Abstract Introduction

Conclusions References

Tables Figures

◀ ▶

◀ ▶

Back Close

Full Screen / Esc

Printer-friendly Version

Interactive Discussion



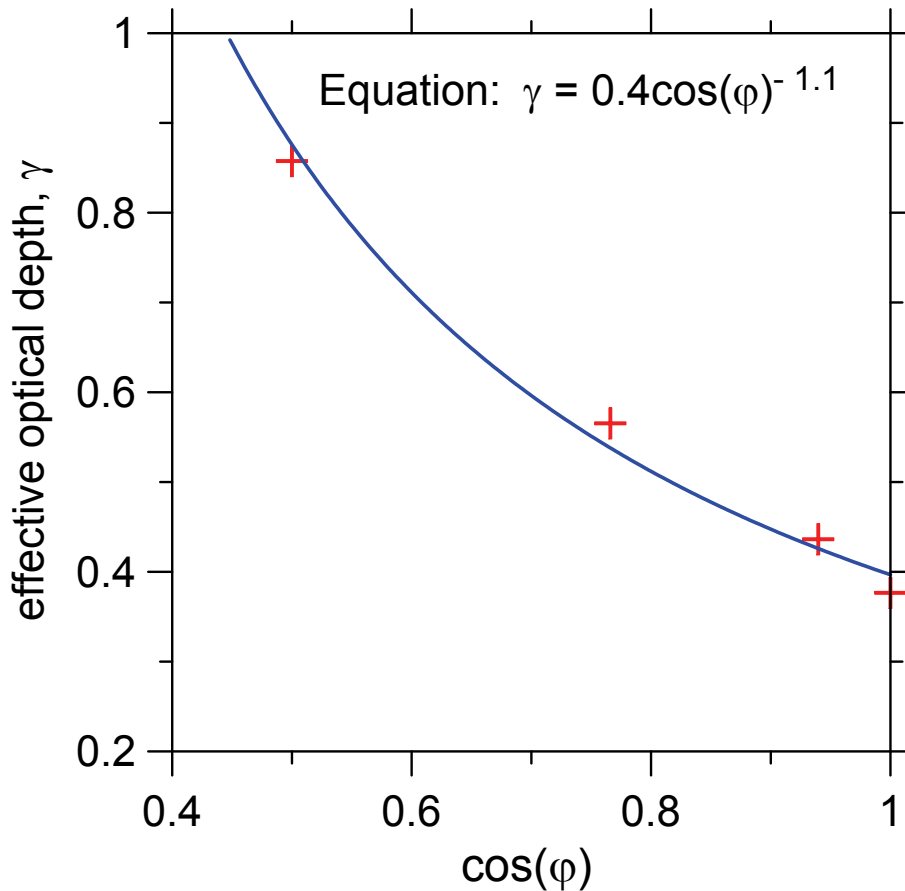


Fig. 2. The dependence of the scaling factor γ (see Eq. 4) on cosine of the solar zenith angle, φ ; crosses: data derived from NO_2 photolysis rate estimates reported by Hodzic et al. (2007); blue line: the approximation used in model simulations in this study (see also an equation shown at the plot).

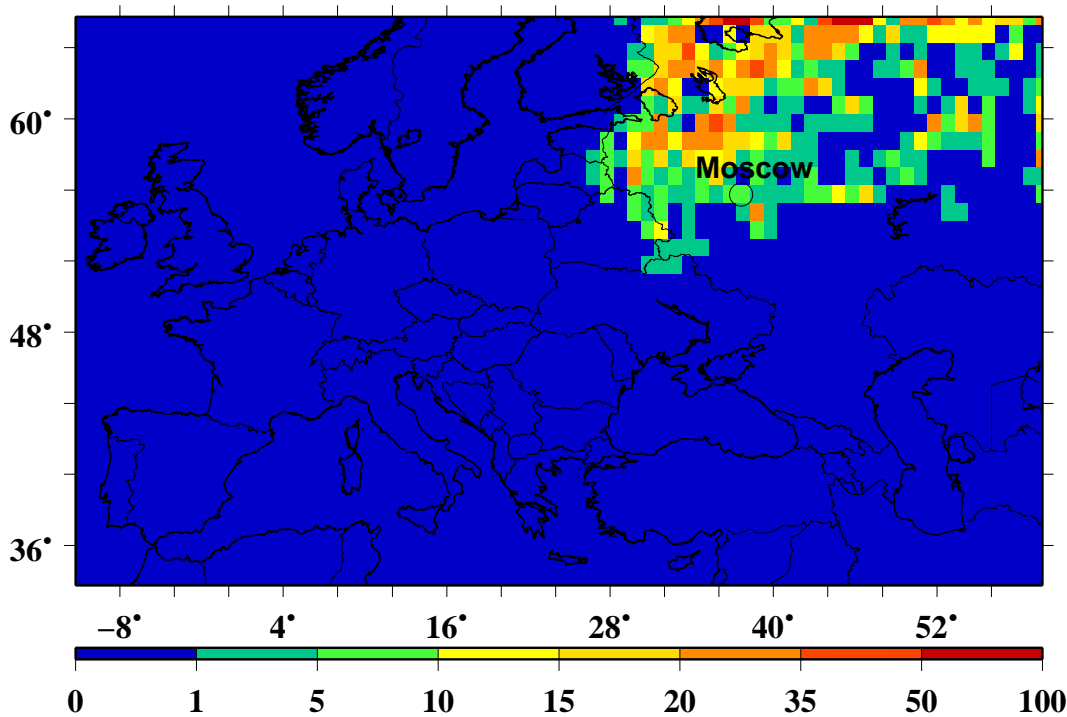


Fig. 3. Fractions (in %) of peat land in a grid cell. Note that the peat land data used in this study are not representative of any country except Russia.

Atmospheric impacts of the 2010 Russian wildfires

I. B. Konovalov et al.

Title Page

Abstract	Introduction
Conclusions	References
Tables	Figures
◀	▶
◀	▶
Back	Close
Full Screen / Esc	
Printer-friendly Version	
Interactive Discussion	



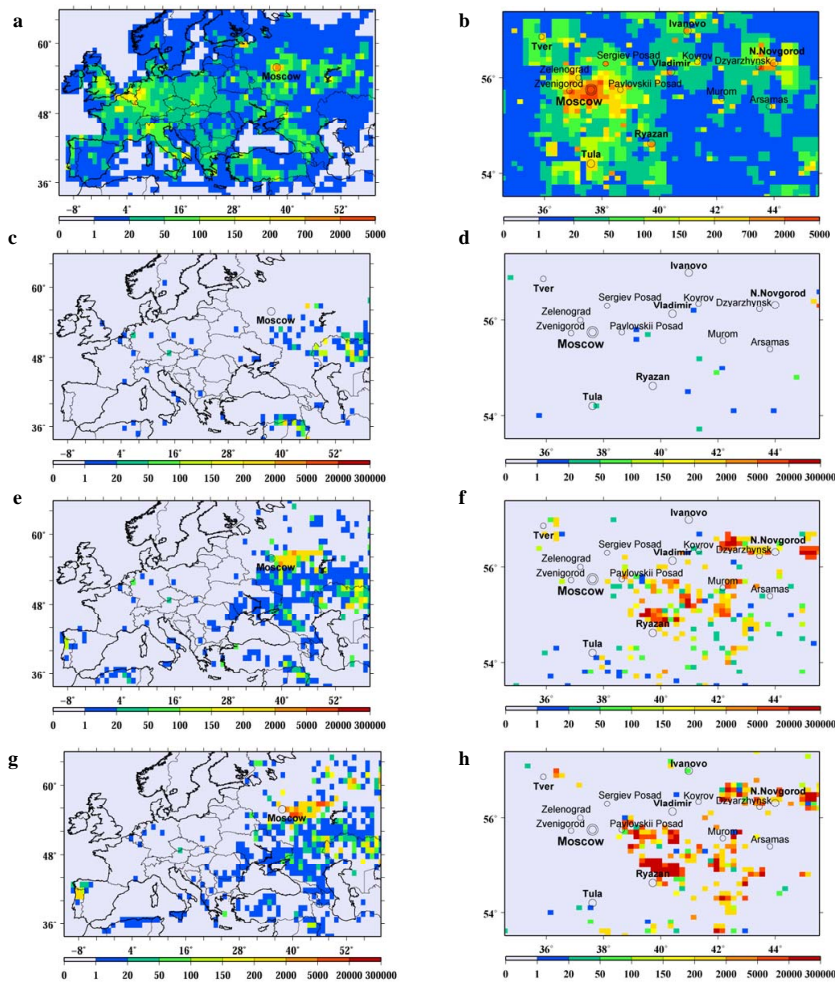


Fig. 5. See caption on next page.

Atmospheric impacts
of the 2010 Russian
wildfires

I. B. Konovalov et al.

Title Page

Abstract

Introduction

Conclusions

References

Tables

Figures

◀

▶

◀

▶

Back

Close

Full Screen / Esc

Printer-friendly Version

Interactive Discussion



**Atmospheric impacts
of the 2010 Russian
wildfires**I. B. Konovalov et al.

[Title Page](#)[Abstract](#)[Introduction](#)[Conclusions](#)[References](#)[Tables](#)[Figures](#)[I◀](#)[▶I](#)[◀](#)[▶](#)[Back](#)[Close](#)[Full Screen / Esc](#)[Printer-friendly Version](#)[Interactive Discussion](#)

Fig. 5. Rates of anthropogenic (**a, b**) and pyrogenic (**c–h**) CO emissions specified in CHIMERE (in 10^{10} molecules/(cm^2 s)). Anthropogenic emissions are averaged over three summer months (June–August) and pyrogenic emissions are presented as averages over June (**c, d**), July (**e, f**), and August (**g, h**). The emission rates are shown separately for a large model domain covering both Western and Eastern Europe with the coarse resolution of $1^\circ \times 1^\circ$ (on the left) and for a small (nested) domain covering only several European regions of Russia with the finer resolution of $0.2^\circ \times 0.1^\circ$ (on the right). Note that the colour palette in the case of pyrogenic emissions is extended.

Atmospheric impacts of the 2010 Russian wildfires

I. B. Konovalov et al.

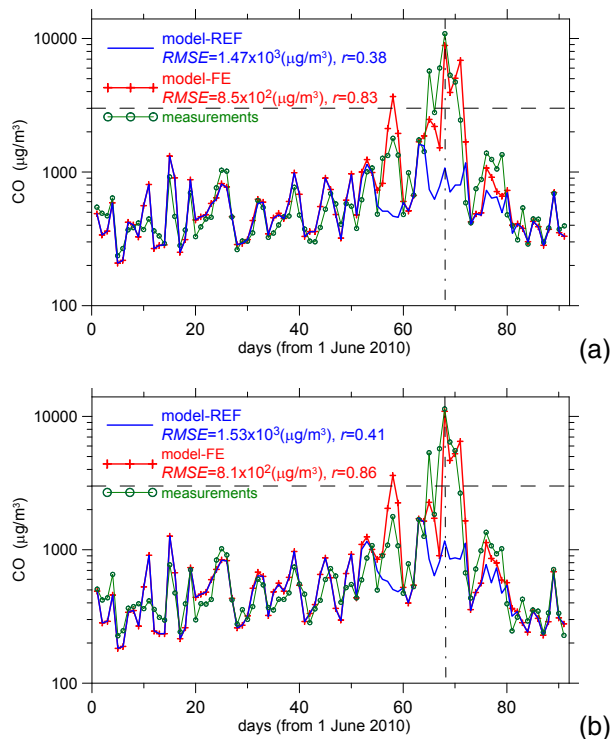


Fig. 6. Daily mean CO concentrations simulated by CHIMERE without (the REF run) and with (the FE run) wildfire emissions in comparison with corresponding measurements. Concentrations are averaged over monitoring sites **(a)** used in optimisation procedure and **(b)** employed only for validation of the modelling results. The dashed horizontal lines depict the threshold CO daily mean concentration defined by the Russian air quality standards, and the vertical dash-dot lines mark the 68th day (7 August). Note that concentrations are given on a logarithmic scale. Note also that although RMSE in the FE case is about as large as typical CO concentrations under normal conditions, it is a factor of ten less than the maximum CO concentration observed during the considered period.

Title Page

Abstract

Introduction

Conclusions

References

Tables

Figures

◀

▶

◀

▶

Back

Close

Full Screen / Esc

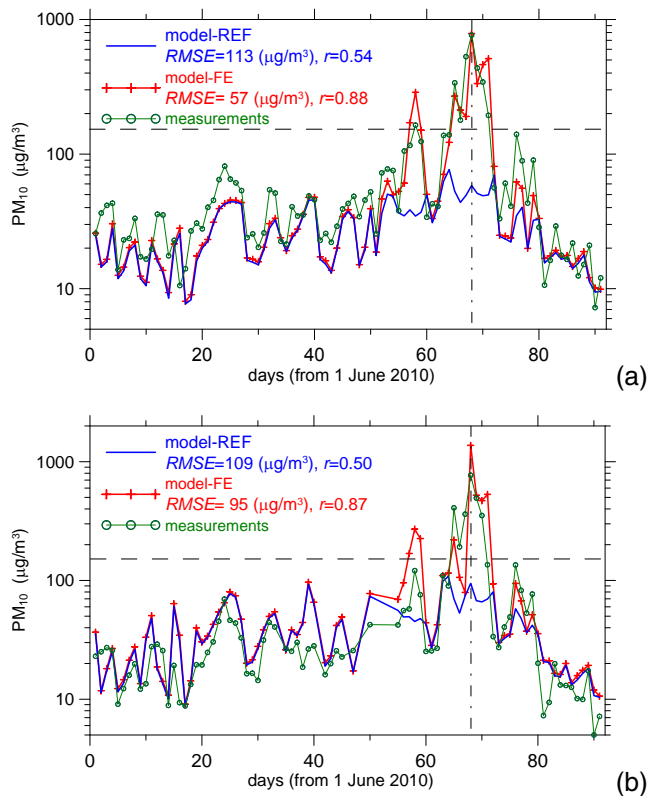
Printer-friendly Version

Interactive Discussion



**Atmospheric impacts
of the 2010 Russian
wildfires**

I. B. Konovalov et al.

**Fig. 7.** The same as in Fig. 6 but for PM_{10} concentrations.

Title Page

Abstract

Introduction

Conclusions

References

Tables

Figures

◀

▶

◀

▶

Back

Close

Full Screen / Esc

Printer-friendly Version

Interactive Discussion



**Atmospheric impacts
of the 2010 Russian
wildfires**

I. B. Konovalov et al.

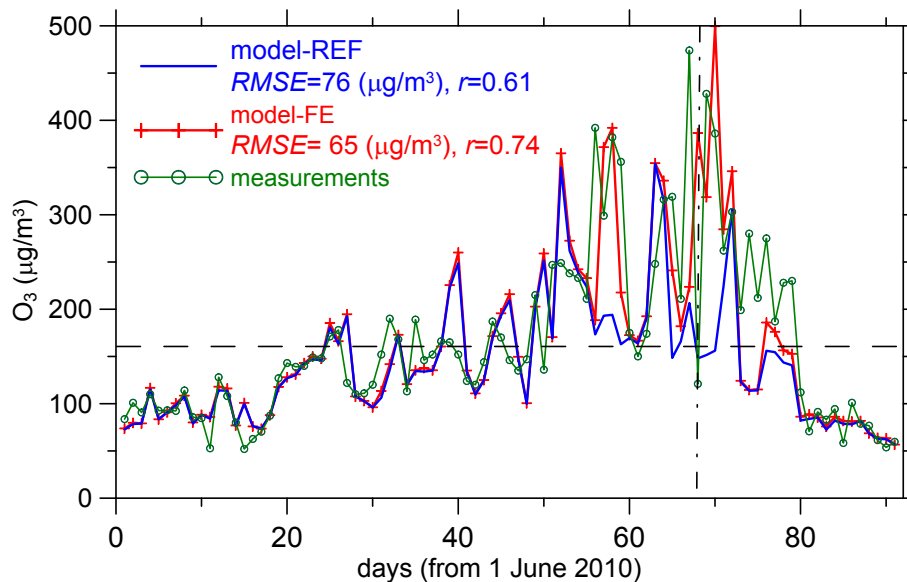


Fig. 8. Daily maximums of ozone concentrations simulated by CHIMERE without (the REF run) and with (the FE run) wildfire emissions in comparison with daily maximums of 1 h average ozone concentrations measured at the sites of Mosecomonitoring in the Moscow region. Each data point represents the largest value among daily maximum ozone concentrations at all of the ozone monitoring sites considered in this study. The dashed horizontal lines depict the threshold O_3 concentration ($160 \mu\text{g m}^{-3}$) defined by the Russian air quality standards, and the vertical dash-dot lines mark the 68th day (7 August).

Title Page

Abstract

Introduction

Conclusions

References

Tables

Figures

◀

▶

◀

▶

Back

Close

Full Screen / Esc

Printer-friendly Version

Interactive Discussion



**Atmospheric impacts
of the 2010 Russian
wildfires**

I. B. Konovalov et al.

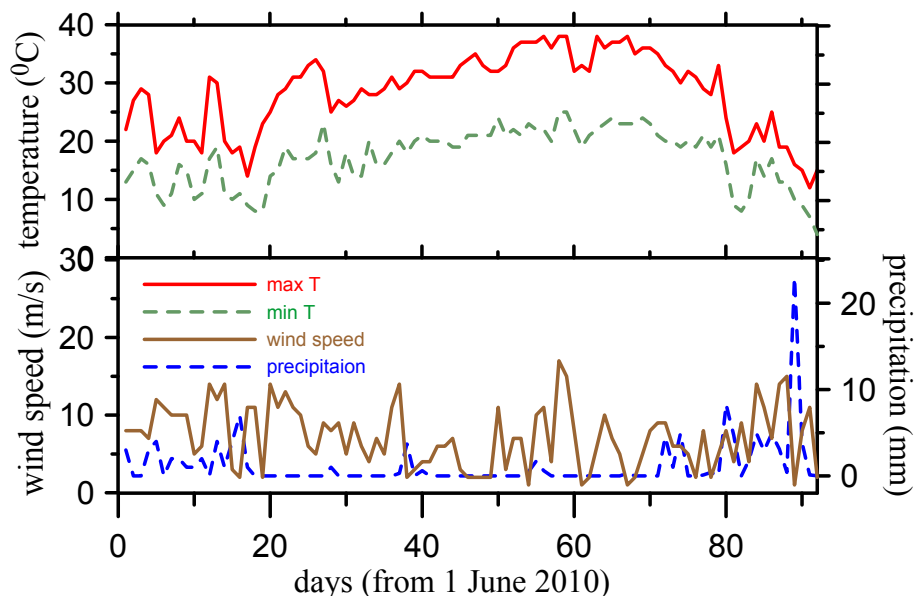


Fig. 9. Measurements of daily maximum and minimum of 2-m temperature (red and green lines at the upper panel) along with wind speed at 925 hPa pressure at 00:00 UT and daily precipitation (brown and blue lines at the lower panel). Wind speed was measured by radiosounding in Moscow, and other data were collected at the meteorological station situated in the Moscow State University.

[Title Page](#)[Abstract](#)[Introduction](#)[Conclusions](#)[References](#)[Tables](#)[Figures](#)[◀](#)[▶](#)[◀](#)[▶](#)[Back](#)[Close](#)[Full Screen / Esc](#)[Printer-friendly Version](#)[Interactive Discussion](#)



Fig. 10. Views of Moscow (Aivazovskogo str., Yasenevo) on 17 June 2010, 20:22 (left) and 7 August 2010, 17:05. Source: 2010 Russian Fires (2010). The picture is reproduced under the terms of the GNU Free Documentation License.

**Atmospheric impacts
of the 2010 Russian
wildfires**

I. B. Konovalov et al.

Title Page

Abstract

Introduction

Conclusions

References

Tables

Figures

◀

▶

◀

▶

Back

Close

Full Screen / Esc

Printer-friendly Version

Interactive Discussion



NOAA HYSPLIT MODEL
 Backward trajectories ending at 2000 UTC 07 Aug 10
 GDAS Meteorological Data

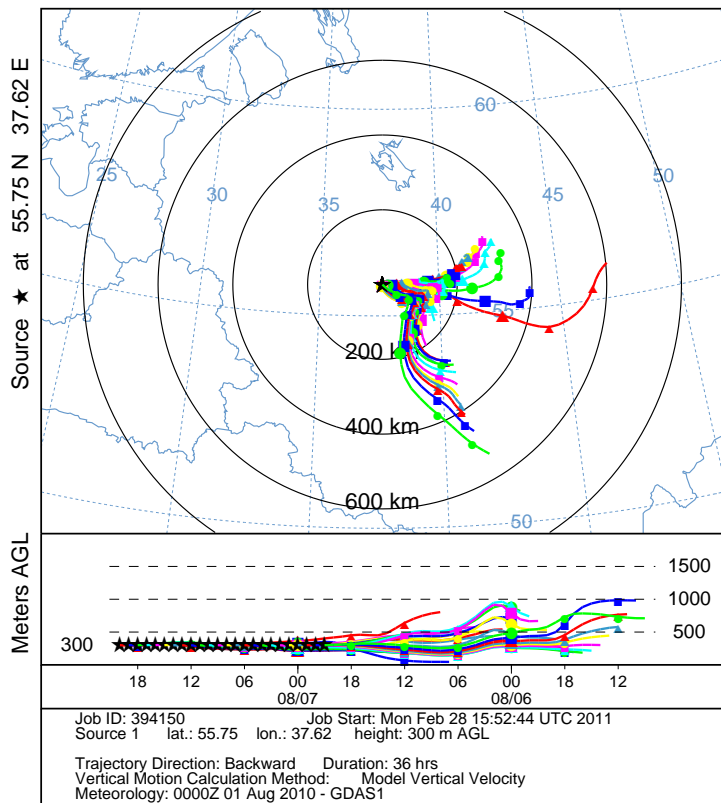


Fig. 11. HYSPLIT backward trajectories ending in Moscow at 7 August 2010. Different trajectories have different arrival time in the range from 6 August, 20:00 UTC to 7 August, 20:00 UTC. Note that 20:00 UTC corresponds to 24:00 LST (local summer time) in Moscow.

Atmospheric impacts
 of the 2010 Russian
 wildfires

I. B. Konovalov et al.

Title Page

Abstract

Introduction

Conclusions

References

Tables

Figures

◀

▶

◀

▶

Back

Close

Full Screen / Esc

Printer-friendly Version

Interactive Discussion



**Atmospheric impacts
of the 2010 Russian
wildfires**

I. B. Konovalov et al.

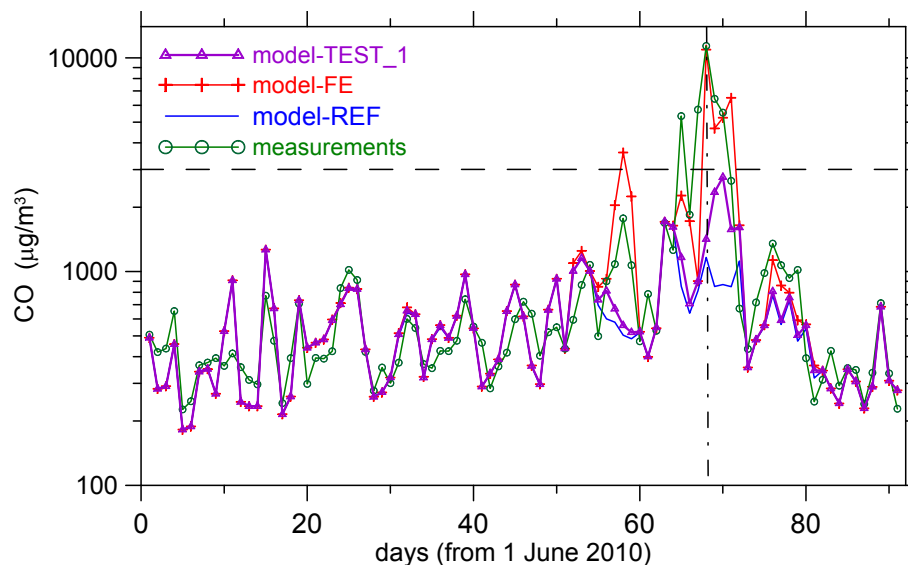


Fig. 12. Daily mean CO concentrations obtained as a result of the TEST_1 simulation where wildfire emissions in a region surrounding Moscow were put to zero (see the text for the region definition) in comparison with concentrations simulated in the FE and REF runs of the model and observed in the validation monitoring sites. Concentrations are averaged over validation subset of monitoring sites. The dashed horizontal line depicts the threshold CO daily mean concentration defined by the Russian air quality standards, and the vertical dash-dot line marks the 68th day (7 August).

Title Page

Abstract

Introduction

Conclusions

References

Tables

Figures

◀

▶

◀

▶

Back

Close

Full Screen / Esc

Printer-friendly Version

Interactive Discussion



**Atmospheric impacts
of the 2010 Russian
wildfires**

I. B. Konovalov et al.

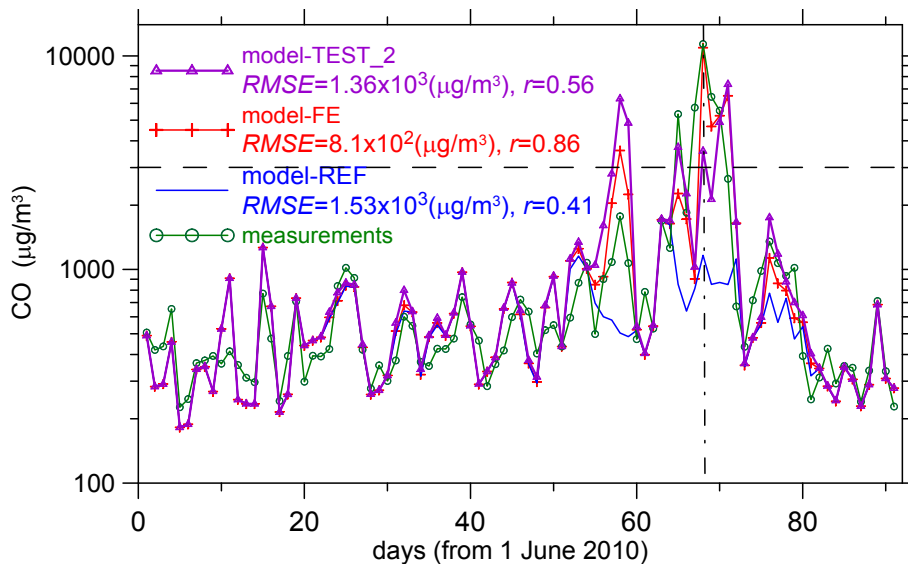


Fig. 13. The same as in Fig. 12 except that the test simulations (the TEST_2 run) were performed with $C(\tau) = 1$ (see Eq. 6).

[Title Page](#)[Abstract](#)[Introduction](#)[Conclusions](#)[References](#)[Tables](#)[Figures](#)[◀](#)[▶](#)[◀](#)[▶](#)[Back](#)[Close](#)[Full Screen / Esc](#)[Printer-friendly Version](#)[Interactive Discussion](#)

Atmospheric impacts of the 2010 Russian wildfires

I. B. Konovalov et al.

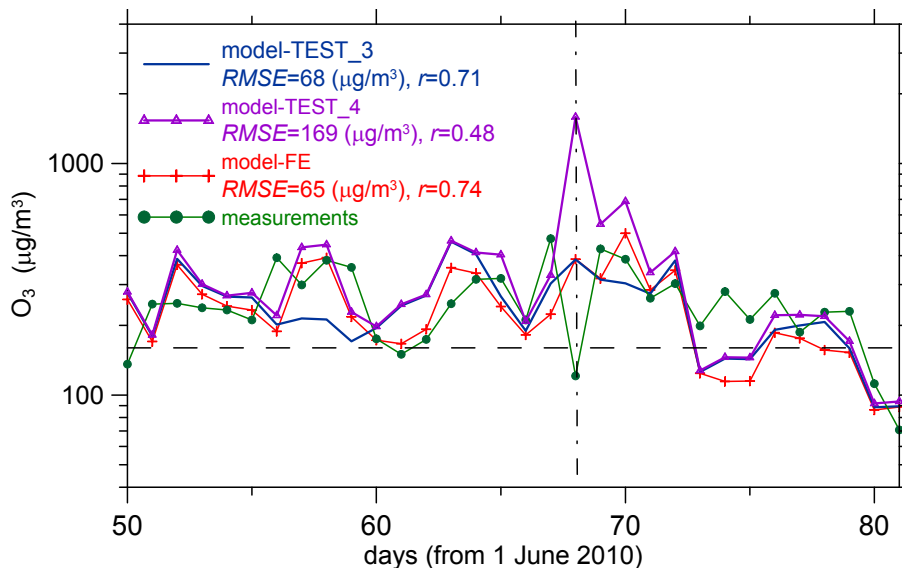


Fig. 14. The same as in Fig. 8, except that instead of results for the REF run, the simulated data are presented for the two test cases (see Table 1 and Sect. 5.3 for definitions). For better readability, only the period most affected by fires is shown (from 20 July to 20 August 2010), although the statistics are evaluated for the whole period considered in this study.

Title Page

Abstract Introduction

Conclusions References

Tables Figures

◀ ▶

◀ ▶

Back Close

Full Screen / Esc

Printer-friendly Version

Interactive Discussion



**Atmospheric impacts
of the 2010 Russian
wildfires**

I. B. Konovalov et al.

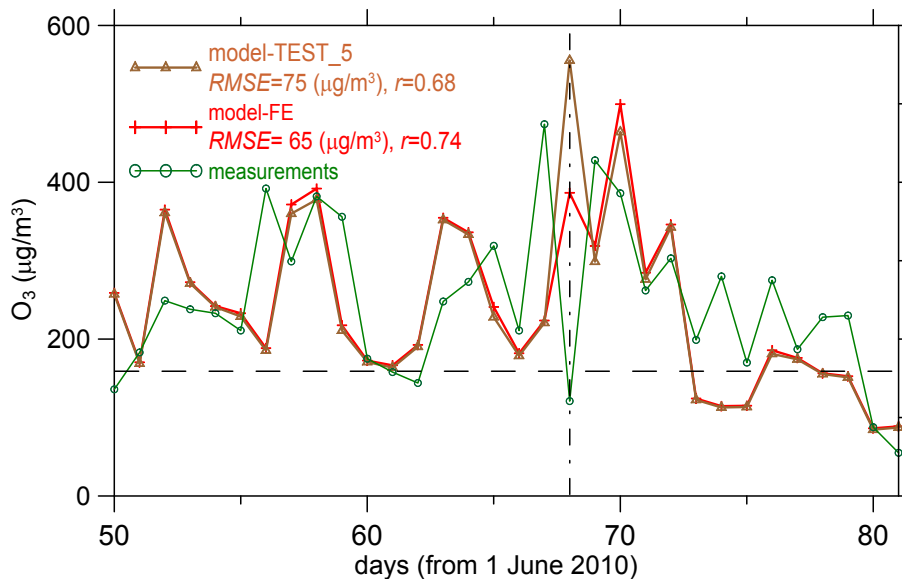


Fig. 15. The same as in Fig. 14, but instead of results for the test cases 3 and 4, the simulated data are presented for the TEST_5 case where heterogeneous reactions specified in the standard version of CHIMERE were taken into account.

[Title Page](#)[Abstract](#)[Introduction](#)[Conclusions](#)[References](#)[Tables](#)[Figures](#)[◀](#)[▶](#)[◀](#)[▶](#)[Back](#)[Close](#)[Full Screen / Esc](#)[Printer-friendly Version](#)[Interactive Discussion](#)

**Atmospheric impacts
of the 2010 Russian
wildfires**

I. B. Konovalov et al.

Title Page

Abstract

Introduction

Conclusions

References

Tables

Figures

◀

▶

◀

▶

Back

Close

Full Screen / Esc

Printer-friendly Version

Interactive Discussion

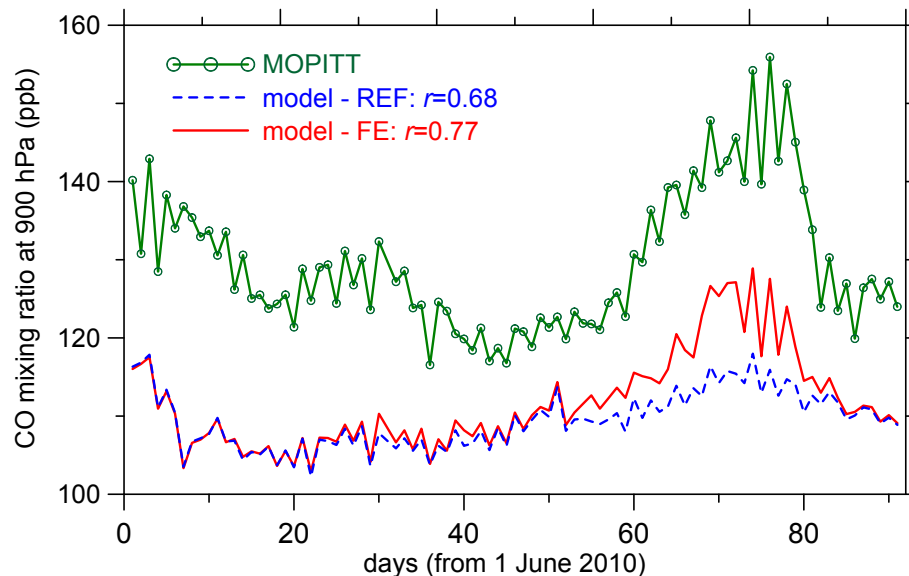


Fig. 16. Comparison of MOPITT CO mixing ratios at the nominal 900 hPa pressure level with corresponding data simulated by CHIMERE with (the FE run) and without (the REF run) fire emissions. The daily data are spatially averaged over the large (European) domain of the model.

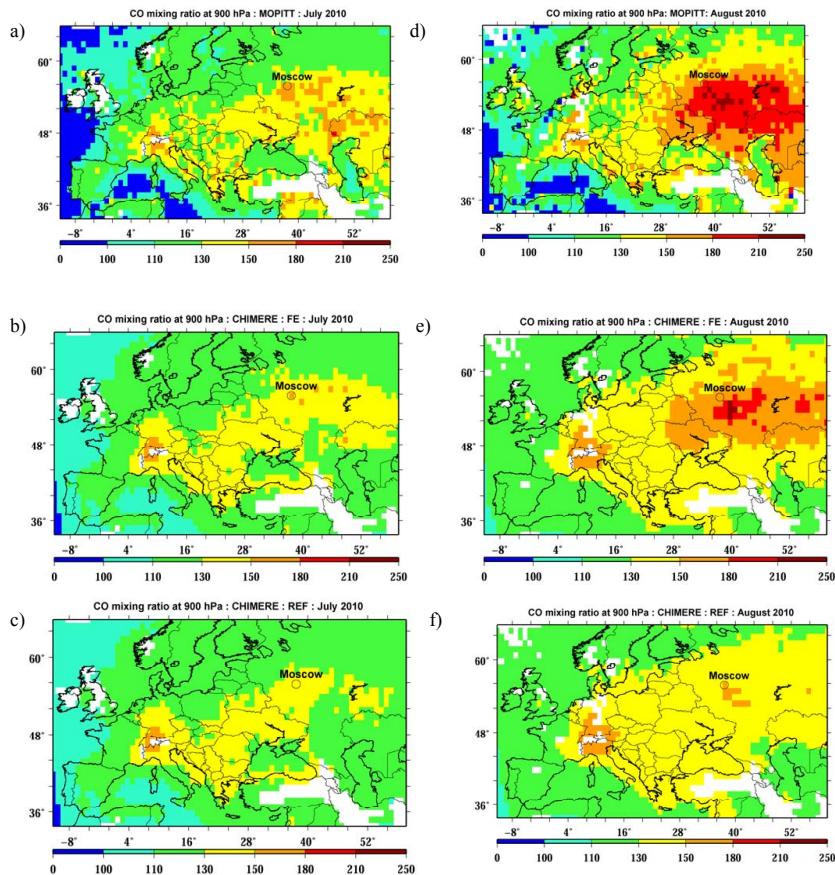


Fig. 17. Spatial distributions of monthly mean CO mixing ratio at the nominal 900 hPa MOPITT pressure level in July (**a–c**) and August (**d–f**) 2010. The MOPITT data (**a, d**) are shown in comparison with simulated CO mixing ratio (corrected for a systematic bias) with (**b, e**) and without (**c, f**) fire emissions.

Atmospheric impacts of the 2010 Russian wildfires

I. B. Konovalov et al.

Title Page

Abstract

Introduction

Conclusions

References

Tables

Figures

◀

▶

◀

▶

Back

Close

Full Screen / Esc

Printer-friendly Version

Interactive Discussion

